cmgh
CELLULAR AND MOLECULAR GASTROENTEROLOGY AND HEPATOLOGY

ORIGINAL RESEARCH

Organic Anion Transporting Polypeptide (OATP) 1B3 is a Significant Transporter for Hepatic Uptake of Conjugated Bile Acids in Humans

Qiong Pan,[1,2,3,*] Guanyu Zhu,[1,2,3,*] Ziqian Xu,[1,2,3,*] Jinfei Zhu,[1,2,3,4,*] Jiafeng Ouyang,[1,2,3] Yao Tong,[1,2,3] Nan Zhao,[1,2,3] Xiaoxun Zhang,[1,2,3] Ying Cheng,[1,2,3] Liangjun Zhang,[1,2,3] Ya Tan,[1,2,3] Jianwei Li,[5] Chengcheng Zhang,[5] Wensheng Chen,[1,2,3] Shi-Ying Cai,[6] James L. Boyer,[6] and Jin Chai[1,2,3]

[1]Department of Gastroenterology, the First Affiliated Hospital (Southwest Hospital), Third Military Medical University (Army Medical University), Chongqing, China; [2]Insitute of Digestive Diseases of PLA, the First Affiliated Hospital (Southwest Hospital), Third Military Medical University (Army Medical University), Chongqing, China; [3]Center for Cholestatic Liver Diseases and Center for Metabolic Associated Fatty Liver Disease, the First Affiliated Hospital (Southwest Hospital), Third Military Medical University (Army Medical University), Chongqing, China; [4]Queen Mary School, Nanchang University, Nanchang, Jiangxi, China; [5]Institute of Hepatobiliary Surgery, Southwest Hospital, Third Military Medical University, Chongqing, China; and [6]Department of Internal Medicine and Liver Center, Yale University School of Medicine, New Haven, Connecticut

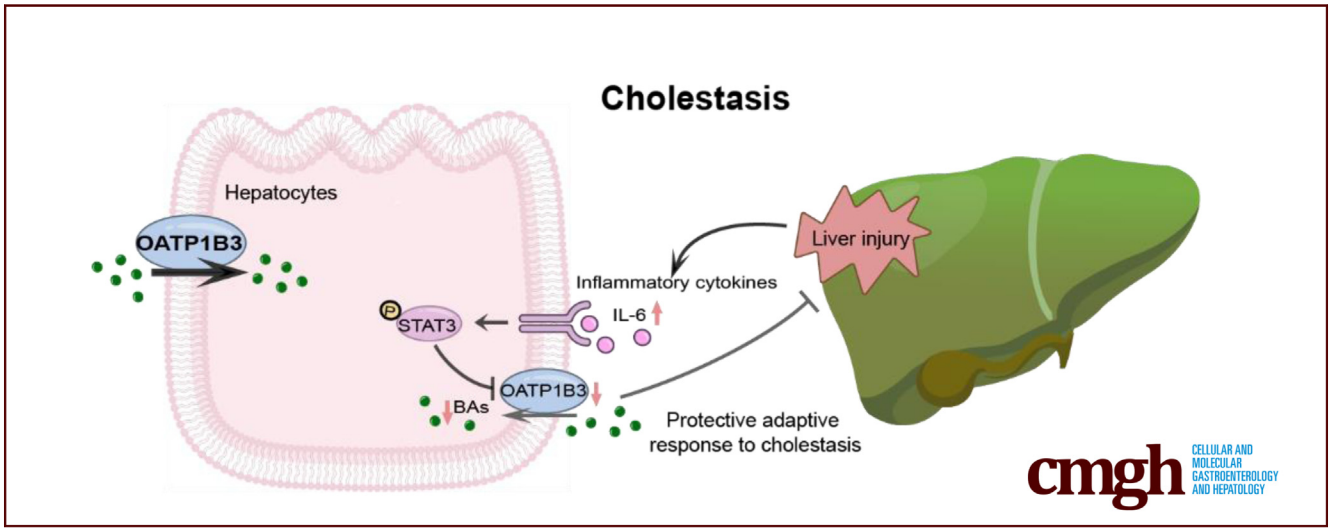

SUMMARY

OATP1B3 functions as a significant transporter for hepatic bile acid uptake and can partially compensate Na+/taurocholate cotransporter for conjugated bile acid uptake. Downregulation of hepatic OATP1B3 is an adaptive protective response against cholestasis.

BACKGROUND & AIMS: OATP1B3/*SLCO1B3* is a human liver-specific transporter for the clearance of endogenous compounds (eg, bile acid [BA]) and xenobiotics. The functional role of OATP1B3 in humans has not been characterized, as *SLCO1B3* is poorly conserved among species without mouse orthologs.

METHODS: *Slc10a1*-knockout (*Slc10a1*$^{-/-}$), *Slc10a1*^{hSLCO1B3} (endogenous mouse *Slc10a1* promoter-driven human-*SLCO1B3* expression in *Slc10a1*$^{-/-}$ mice), and human *SLCO1B3* liver-specific transgenic (*hSLCO1B3*-LTG) mice were generated and challenged with 0.1% ursodeoxycholic-acid (UDCA), 1% cholic-acid (CA) diet, or bile duct ligation (BDL) for functional studies. Primary hepatocytes and hepatoma-PLC/RPF/5 cells were used for mechanistic studies.

RESULTS: Serum BA levels in *Slc10a1*$^{-/-}$ mice were substantially increased with or without 0.1% UDCA feeding compared with wild-type (WT) mice. This increase was attenuated in *Slc10a1*^{hSLCO1B3}-mice, indicating that OATP1B3 functions as a significant hepatic BA uptake transporter. *In vitro* assay using primary hepatocytes from WT, *Slc10a1*$^{-/-}$, and *Slc10a1*^{hSLCO1B3}-mice indicated that OATP1B3 has a similar capacity in taking up taurocholate/TCA as Ntcp. Furthermore, TCA-induced bile flow was significantly impaired in *Slc10a1*$^{-/-}$ mice but partially recovered in *Slc10a1*^{hSLCO1B3}-mice, indicating that OATP1B3 can partially compensate the NTCP function in vivo. Liver-specific overexpression of OATP1B3 markedly increased the level of

hepatic conjugated BA and cholestatic liver injury in 1% CA-fed and BDL mice. Mechanistic studies revealed that conjugated BAs stimulated Ccl2 and Cxcl2 in hepatocytes to increase hepatic neutrophil infiltration and proinflammatory cytokine production (eg, IL-6), which activated STAT3 to repress OATP1B3 expression by binding to its promoter.

CONCLUSIONS: Human OATP1B3 is a significant BA uptake transporter and can partially compensate Ntcp for conjugated BA uptake in mice. Its downregulation in cholestasis is an adaptive protective response. *(Cell Mol Gastroenterol Hepatol 2023;16:223–242; https://doi.org/10.1016/j.jcmgh.2023.04.007)*

Keywords: Bile Acid Transporter; Cholestasis; OATP1B3; Proinflammatory Cytokine.

See editorial on page 319.

The liver is responsible for the clearance of both endogenous and foreign compounds from blood, a process depending on members of the organic anion transporting polypeptide (OATP) and other transporter families.[1-6] There are 11 members in the OATP family in humans,[3] and many of them are human specific without mouse orthologs, such as *SLCO1B3*/OATP1B3 (previously called OATP-8 or LST2).[3-6] OATP1B3 is a liver-specific protein and expressed on the basolateral membrane of hepatocytes in humans.[3-6] Although many OATPs share a wide range of substrates, including bilirubin, bile acids (BAs), hormone conjugates, and many drugs, OATP1B3 can also transport some unique substrates, such as cholecystokinin 8 and some drugs.[3-8] However, the functional significance of hepatic OATP1B3 in health and liver diseases remains unclear.

Although mutations of OATP1B3 alone have not been directly associated with any diseases, deficiency of both OATP1B3 and OATP1B1 (*SLCO1B1*) results in Rotor syndrome, a hereditary cause of hyperbilirubinemia.[9] Moreover, *SLCO1B3* polymorphisms have been linked with the variation in metabolism of many drugs.[5] The *SLC10A1* encodes the sodium taurocholate cotransporting polypeptide (NTCP). Its functional deficiency is associated with hypercholanemia,[10-12] indicating its key role in maintaining BA homeostasis. Interestingly, the levels of OATP1B3, as well as NTCP, are down-regulated in the liver of patients with progressive familial intrahepatic cholestasis type 2 and 3 (PFIC-2 and -3), primary biliary cholangitis (PBC), and/or in the placenta of patients with intrahepatic cholestasis of pregnancy (ICP),[13,14] suggesting they play a role in these diseases. The functional role of NTCP in hepatic BA uptake has been well characterized. However, little is known about the function and expression regulation of human OATP1B3 in physiological and cholestatic conditions.

During cholestasis, accumulated intrahepatic BAs stimulate the production of pro-inflammatory cytokines and chemokines that recruit inflammatory cells, resulting in deteriorating cholestatic liver injury.[15] Elevated levels of pro-inflammatory cytokines, such as interleukin 6 (IL-6), IL-1β, and tumor necrosis factor-alpha (TNFα), are detected in bile duct-ligated (BDL) mice and patients with obstructive cholestasis (OC).[16,17] Interestingly, treating human hepatocytes in vitro with IL-6 or TNFα decreases OATP1B3 and NTCP expression in these cells.[18] Furthermore, IL-6 can bind to the receptors IL-6R/gp130 and activate the downstream JAKs/STAT3 (the signal transducer and activator of transcription 3), which regulates cell proliferation, angiogenesis, inflammation, and immune responses.[19] Recent studies have reported that enhanced STAT3 activation is detected in the liver of lithocholic acid-induced cholestatic mice, and the STAT3 activation ameliorates sepsis-induced liver injury in rats.[20,21] Our previous study revealed that hepatic STAT3 phosphorylation was increased in cholestatic patients.[22] However, it remains unceretain if IL-6/STAT3 signaling modulates OATP1B3 expression in human cholestasis.

To investigate the functional significance of OATP1B3 in physiological and cholestatic conditions, we employed 3 genetic mouse models (ie, *Slc10a1*$^{-/-}$ [knockout of *Slc10a1* gene], *Slc10a1*^{hSLCO1B3} [endogenous mouse *Slc10a1* promoter-driven human *SLCO1B3* expression in *Slc10a1*$^{-/-}$ mice] and *hSLCO1B3*-LTG [liver-specific overexpression of human *SLCO1B3*] mice). We also analyzed specimens from human patients. Our results indicate that OATP1B3 is an important BA uptake transporter in the liver and can partially compensate for Ntcp-dependent BA uptake in mice. Downregulation of OATP1B3 in human cholestasis should function as an adaptive protective response.

Results

Human OATP1B3 Replaces the Function of Ntcp for Conjugated BA Uptake in Mice

To assess the functional role of hepatic OATP1B3 in vivo, *Slc10a1*$^{-/-}$ (Figure 1*A–B*) and *Slc10a1*^{hSLCO1B3} mice (Figure 1*C–D*) were generated. Hepatic Ntcp and OATP1B3 protein expression in these mice were assayed using Western blot (Figure 1*E*). Creation of these 2 strains of mice eliminates the potential interference of Ntcp in assessing BA uptake, providing a cleaner background for determination of

***Authors share co-first authorship.**

Abbreviations used in this paper: **ALP, alkaline phosphatase; ALT, alanine aminotransferase; AST, aspartate aminotransferase; BA, bile acid; BDL, bile duct-ligated; CA, cholic acid; CDCA, chenocholic acid; ChIP, chromatin immunoprecipitation; DCA, deoxycholic acid; GCA, glycocholate acid; hSLCO1B3 LTG mice, human OATP1B3 liver-specific transgenic mice; ICP, intrahepatic cholestasis of pregnancy; IL, interleukin; LC-MS/MS, liquid chromatography/tandem mass spectrometry; MCA, muricholic acid; NTCP, sodium taurocholate cotransporting polypeptide; OATP, organic anion-transporting polypeptide; OC, obstructive cholestasis; PBC, primary biliary cholangitis; PFIC-2 and -3, progressive familial intrahepatic cholestasis type 2 and 3; RT-qPCR, real-time quantitative polymerase chain reaction; TBA, total bile acid; TCA, taurocholic acid; TCDCA, taurochenodeoxycholate acid; TDCA, taurodeoxycholate acid; TMCA, tauromuricholate acid; TNFα, tumor necrosis factor-alpha; UDCA, ursodeoxycholic acid; WT, wild-type.**

Most current article

2352-345X
https://doi.org/10.1016/j.jcmgh.2023.04.007

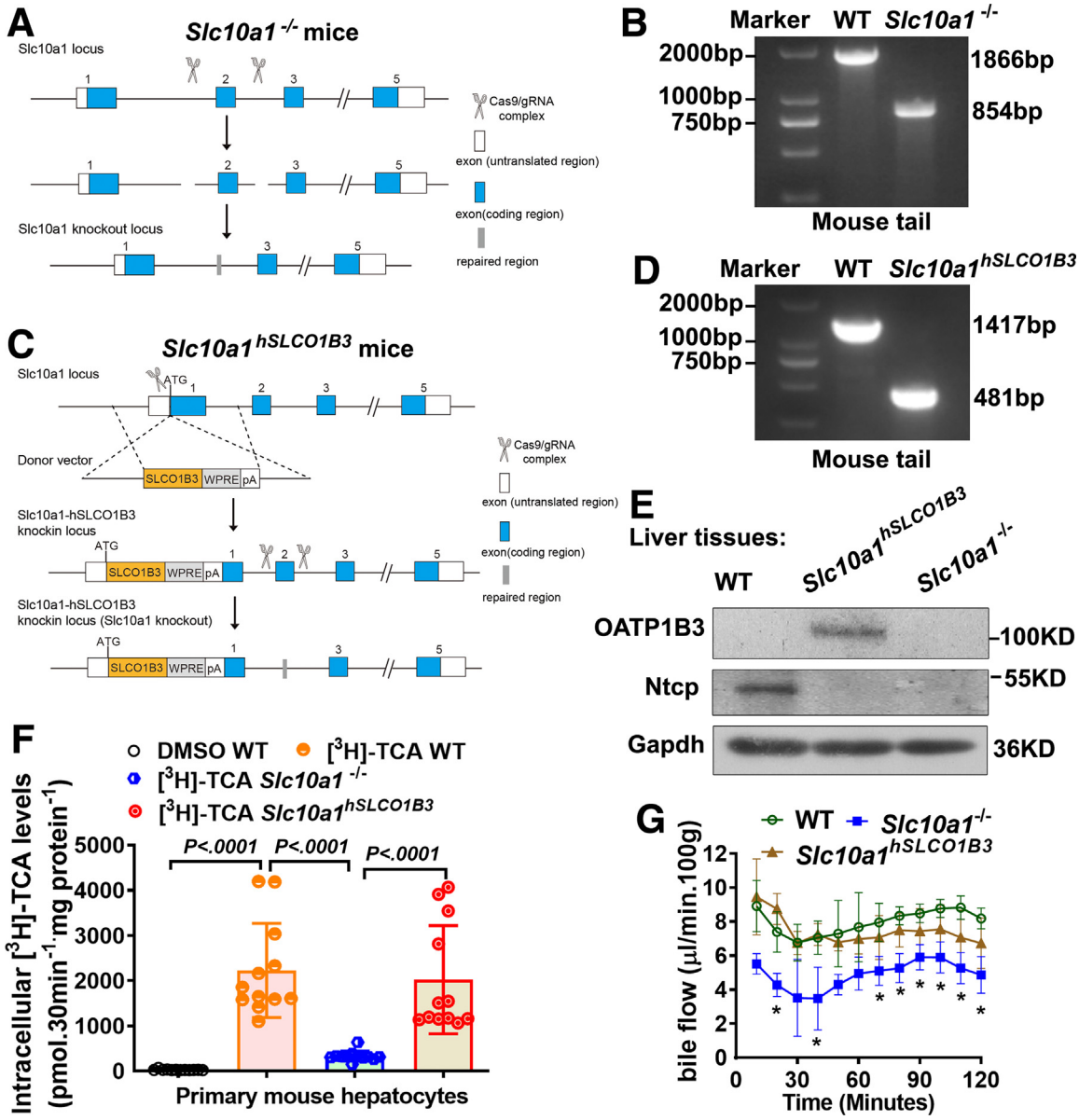

Figure 1. Generation and characterization of *Slc10a1*$^{-/-}$ and *Slc10a1*^{hSLCO1B3} mice. (*A*) A schematic diagram of the strategy for generation of *Slc10a1*$^{-/-}$ mice. (*B*) Genotyping of *Slc10a1*$^{-/-}$ mice. Genomic DNA was extracted from mouse tails and analyzed by PCR, followed by agarose gel electrophoresis. (*C*) A schematic diagram of the strategy for generation of *Slc10a1*^{hSLCO1B3} mice. (*D*) Genotyping of *Slc10a1*^{hSLCO1B3} mice. (*E*) Western blot analysis of the expression of OATP1B3 and Ntcp in different strains of mice. (*F*) The levels of intracellular [^{3}H]-TCA in primary hepatocytes from WT, *Slc10a1*$^{-/-}$, and *Slc10a1*^{hSLCO1B3} mice were analyzed by [^{3}H]-TCA uptake after these cells were treated with 1 pM [^{3}H]-TCA for 30 min (n = 12 per group). (*G*) Bile flow was measured in WT, *Slc10a1*$^{-/-}$, and *Slc10a1*^{hSLCO01B3} mice with the tail vein injection of TCA. Bile samples were collected every 10 minutes and continued for up to 120 minutes following TCA (30μmol/L) infusion (n = 3 per each group). *$P < .05$ vs the WT group at the same timepoint. *Slc10a1*$^{-/-}$, *Slc10a1* knockout mice; *Slc10a1*^{hSLCO1B3}, *Slc10a1*$^{hSLCO1B3/hSLCO1B3}$*Slc10a1*$^{-/-}$ homozygous mice with both endogenous *Slc10a1* promoter-driven human *SLCO1B3* expression and *Slc10a1* knockout; WT, wild-type C57BL/6 mice.

OATP1B3's substrate specificity for BA. Next, these mice were fed with regular chow or chow containing 0.1% ursodeoxycholic acid (UDCA) for 14 days to stimulate hepatic BA uptake. When fed with regular chow, the levels of serum and liver total bile acids (TBA) in the *Slc10a1*$^{-/-}$ mice were significantly higher than in wild-type (WT) controls, consistent with a previous report,[10] but this elevation was diminished in the *Slc10a1*^{hSLCO1B3} mice (Table 1). Similarly, when fed with 0.1% UCDA diet for 14 days, it was notable that, compared with WT mice, the levels of serum and liver TBA were substantially elevated in *Slc10a1*$^{-/-}$ mice, which was abolished in *Slc10a1*^{hSLCO1B3} mice, although the levels of

Table 1. Serum Biochemistry in 8-week-old Mice Fed With 0.1% UDCA for 14 Days

Liver function tests	Chow diet, 14 days			0.1% UDCA diet, 14 days		
	WT (n = 10)	*Slc10a1*$^{-/-}$ (n = 7)	*Slc10a1*^{hSLC01B3} (n = 8)	WT (n = 8)	*Slc10a1*$^{-/-}$(n = 8)	*Slc10a1*^{hSLC01B3} (n = 8)
ALT, *IU/L*	13.22 ± 1.09	25.14 ± 1.84	14.23 ± 1.14	21.28 ± 2.76	163.00 ± 90.79[c]	15.03 ± 2.72[d]
AST, *IU/L*	88.64 ± 7.01	63.86 ± 6.20	57.93 ± 6.49	74.25 ± 5.07	227.00 ± 98.04	61.95 ± 5.97[d]
ALP, *IU/L*	53.20 ± 1.91	84.86 ± 8.56[a]	46.50 ± 3.76[b]	36.00 ± 1.25	51.20 ± 6.85	51.25 ± 6.02
TBA, *μmol/L*	3.16 ± 0.60	60.46 ± 54.58[a]	9.30 ± 4.65	3.93 ± 0.34	445.06 ± 96.16[c]	8.42 ± 3.07[d]
Total liver bile salt, *μmol/kg of liver)*	179.50 ± 29.53	366.00 ± 44.78[a]	181.90 ± 29.47[b]	205.50 ± 33.75	544.9 ± 52.83[c]	213.60 ± 25.96[d]

Note: Values are mean ± standard error of the mean.
Note: The data were analyzed by 1-way analysis of variance with Tukey's post hoc tests or by non-parametric test with Mann-Whitney *U* test.
ALP, Alkaline phosphatase; ALT, alanine aminotransferase; AST, aspartate aminotransferase; TBA, total bile acids; *Slc10a1*$^{-/-}$, *Slc10a1* knockout mice; *Slc10a1*^{hSLCO1B3}, *Slc10a1*$^{hSLCO1B3/hSLCO1B3}$*Slc10a1*$^{-/-}$ homozygous mice with both *Slc10a1* promoter-driven human *SLCO1B3* expression and *Slc10a1* knockout; UDCA, ursodeoxycholic acid; WT, wild-type C57BL/6 mice.
[a]$P < .05$ vs WT mice with chow diet.
[b]$P < .05$ vs *Slc10a1*$^{-/-}$ mice with chow diet.
[c]$P < .05$ vs WT mice with 0.1% UDCA diet.
[d]$P < .05$ vs *Slc10a1*$^{-/-}$ mice with 0.1% UDCA diet.

serum and liver TBA in *Slc10a1*^{hSLCO1B3} mice remained slightly higher than WT mice (Table 1). There was no significant difference in the levels of serum alanine aminotransferase (ALT), aspartate aminotransferase (AST), and alkaline phosphatase (ALP) between WT and *Slc10a1*^{hSLCO1B3} mice with or without 0.1% UDCA diet feeding (Table 1).

To further confirm our in vivo observations, primary hepatocytes were isolated from WT, *Slc10a1*$^{-/-}$, and *Slc10a1*^{hSLCO1B3} mice and exposed to [^{3}H]-labeled taurocholic acid (TCA) for 30 minutes. Significant increases in the level of intracellular [^{3}H]-TCA were detected in this assay in WT primary hepatocytes, but not in *Slc10a1*$^{-/-}$ primary hepatocytes, which were rescued in *Slc10a1*^{hSLCO1B3} primary hepatocytes (Figure 1*F*). Together, these findings demonstrate that OATP1B3 is a key transporter for hepatic BA uptake, with a function similar to Ntcp for [^{3}H]-TCA uptake in mouse primary hepatocytes. Next, we measured bile flow in WT, *Slc10a1*$^{-/-}$, and *Slc10a1*^{hSLCO1B3} mice by tail vein infusion of TCA. We found that TCA-induced bile flow seen in WT and *Slc10a1*^{hSLCO1B3} mice was impaired in *Slc10a1*$^{-/-}$ mice (Figure 1*G*), whereas no significant difference in bile flow between WT and *Slc10a1*^{hSLCO1B3} mice (Figure 1*G*). Moreover, liquid chromatography/tandem mass spectrometry (LC-MS/MS) analysis of BA compositions in collected bile demonstrated that the levels of conjugated BA taurochenodeoxycholate acid (TCDCA) were significantly lower in *Slc10a1*$^{-/-}$ mice when compared with WT and *Slc10a1*^{hSLCO1B3} mice after TCA injection (Table 2). These data support the notion that human OATP1B3 functions as a significant BA uptake transporter, because it can partially compensate for the function of Ntcp, the major BA uptake transporter in mice.

Human OATP1B3 Liver-specific Overexpression Significantly Increases Intrahepatic Conjugated BAs and Cholestatic Liver Injury in 1% CA-fed and BDL Mice

Because the expression of OATP1B3 is down-regulated in several cholestatic diseases, such as PIFC-2/3, PBC and ICP,[13,14] we speculated that this down regulation served as an adaptive protective response. To verify whether this is the case, we generated *hSLCO1B3* LTG mice, where the expression of *hSLCO1B3* was controlled by mouse albumin promoter, but not the *Slc10a1* promoter (Figure 2*A–C*). When these *hSLCO1B3* LTG mice were maintained on a regular chow diet, serum biochemistry analyses revealed that they had significantly higher levels of serum ALT and AST, but lower TBA than in the WT controls (Table 3). Of note, all these numbers remained in the normal physiological range, and there was no histologic change (data not shown). However, when these mice were challenged with 1% cholic acid (CA) feeding for 14 days, cholestatic liver injury developed as expected, and serum levels of TBA, ALT, AST, and ALP significantly increased when compared with regular chow-fed animals. Higher levels of hepatic total bile salts and serum levels of ALT and AST were found in *hSLCO1B3* LTG mice after 1% CA feeding compared with the WT controls, although serum levels of ALP and TBA remained similar between these 2 groups (Table 3). Together, these findings in mice suggest that the down regulation of human OATP1B3 in cholestasis may also protect hepatocytes from BA-induced liver injury in human cholestasis.

Because OATP1B3 is a multi-specific organic anion transporter, we determined which compounds were its in vivo substrates and might contribute to cholestatic liver injury. For example, tauromuricholate acid (TMCA), TCA, TCDCA, and taurodeoxycholate acid (TDCA) in 1% CA-fed

Table 2. Bile Salt Composition of bile in WT, *Slc10a1*$^{-/-}$, and *Slc10a1*^{hSLC01B3} Mice With the Tail Vein Injection of TCA

	WT		*Slc10a1*$^{-/-}$		*Slc10a1*^{hSLC01B3}	
Bile acid types	$t = 0$	$t = 120$	$t = 0$	$t = 120$	$t = 0$	$t = 120$
Conjugated BAs, *ng/mL*						
TCDCA	372,309 ± 22,568	328,808 ± 40,346	346,446 ± 55,036	170,180 ± 1887[b,c]	314,212 ± 88,776	228,608 ± 77,317
TDCA	309,974 ± 58,124	186,205 ± 76,275	489,639 ± 116,825	228,608 ± 73,026	275,529 ± 27,991	240,661 ± 5890
TCA	288,279 ± 72,201	271,499 ± 48,430	241,676 ± 19,532	259,549 ± 25,957	256,263 ± 53,566	260,479 ± 51,291
Tω-MCA	19,429 ± 7788	18,825 ± 5605	8434 ± 2013	13,844 ± 2675	25,480 ± 8388	19,065 ± 9085
Unconjugated BAs, *ng/mL*						
CDCA	70 ± 19	33 ± 1	120 ± 72	49 ± 6	366 ± 165	260 ± 174
DCA	142 ± 31	45 ± 15[a]	179 ± 47	52 ± 16	101 ± 6	90 ± 10
CA	12,204 ± 8848	5118 ± 3669	44,067 ± 28,902	12,025 ± 6884	56,774 ± 24,987	68,242 ± 42,089
ω-MCA	21,088 ± 3519	17,282 ± 4545	69,263 ± 45406	26,135 ± 16,129	31,113 ± 14,419	31,931 ± 15,645

Note: Data are presented as mean ± standard deviation.
Note: The data were analyzed by 1-way analysis of variance with Tukey's post hoc tests or by non-parametric test with Mann-Whitney *U* test. n = 3 for each group.
CA, Cholic acid; CDCA, chenodeoxycholic acid; DCA, deoxycholic acid; TCA, taurocholic acid; TCDCA, taurochenodeoxycholic acid; TDCA, taurodeoxycholic acid; Tω-MCA, tauro-ω-muricholic acid sodium salt; ω-MCA, ω-muricholic acid sodium salt; WT, wild-type.
[a]$P < .05$ vs WT(t = 0).
[b]$P < .05$ vs WT(t = 120).
[c]$P < .05$ vs *Slc10a1*$^{-/-}$ (t = 0).

hSLCO1B3 LTG liver were 4.36, 3.93, 1.83, and 3.8-fold higher than that of the 1% CA-fed WT controls (Figure 2*D*). In contrast, the levels of unconjugated BAs (muricholic acid [MCA], CA, chenocholic acid [CDCA], and deoxycholic acid [DCA]) were lower in 1% CA-fed *hSLCO1B3* LTG liver than in 1%CA-fed WT controls (Figure 2*E*), despite the higher TBA levels in 1% CA-fed *hSLCO1B3* LTG livers (Table 3). These findings suggest that OATP1B3 overexpression dose not directly affect BA excretion, but enhances conjugated BA uptake, resulting in accumulation of intrahepatic conjugated BAs and thereby aggravating cholestatic liver injury in the 1% CA-fed mice.

Similar changes of serum ALT, AST, ALP, and TBA levels were detected in WT and *hSLCO1B3* LTG mice 3 days after BDL or Sham operation (Table 4). In this experiment, the levels of hepatic TBAs in the BDL-*hSLCO1B3* LTG mice were significantly higher than that in the BDL-WT mice (Table 4). Notably, the gross appearance of livers in *hSLCO1B3* LTG mice appeared rougher and more necrotic than those from WT mice after BDL (Figure 3*A*). Liver histologic assessments confirmed that BDL significantly induced liver necrosis in both WT and *hSLCO1B3* LTG mice, accompanied by increased inflammatory, necrotic, bile duct proliferation, and fibrotic scores (Figure 3 (*B–C*)). Interestingly, more extensive liver necrosis was detected in *hSLCO1B3* LTG mice compared with WT mice after BDL (Figure 3*B–C*). These findings further confirmed that human OATP1B3 overexpression increased hepatic BA accumulation and deteriorated cholestatic liver injury in BDL-induced cholestatic mice.

Human OATP1B3 Overexpression in Cholestatic Mice Disturbs Hepatic Expression of Genes Involved in the Adaptive Response to Cholestasis

To gain insights into why human OATP1B3 overexpression exacerbated cholestatic liver injury, we analyzed the expression of genes involved in maintaining hepatic BA homeostasis and drug metabolism. As shown in (Figure 4*A–F*), although mRNA expression of many genes involved in the adaptive response to cholestasis were altered in both BDL groups, as previously reported,[1,2,23] the mRNA levels of *Mrp2, Mdr1a, Mrp3, Ostα, Cyp3a11,* and *Shp* were significantly lower in the BDL-*hSLCO1B3* LTG group than in the BDL-WT group. In contrast, the mRNA levels of *Ntcp* and *Cyp7a1* were significantly higher in BDL-*hSLCO1B3* LTG mice, whereas there were no significant differences between the groups in hepatic expression of genes related to inflammatory cytokines (*Tnfα, Il-1β, Il-6, Icam-1,* and *Mcp-1)*, fibrosis (*α-SMA, Col1a1, Col1a2, Mmp2,* and *Tgfβ1-3*), bile duct proliferation (*Ck19*), and nuclear receptors (*Fxr, Rxrα,* and *Rarα*). Gene mRNA expression analysis revealed similar alterations in 1% CA-fed mouse livers. There were lower levels of *Mrp2, Mdr1a, Ostα, Ostβ,* and *Cyp3a11* mRNA transcripts, but higher levels of *Ntcp* and *Tnfα*, *Il-1β*, *Il-6*, *Mcp1*, *α-SMA*, *Cola1*, and *Tgfβ1* mRNA transcripts in 1% CA-fed *hSLCO1B3* LTG mouse livers than in 1% CA-fed WT mouse livers (Figure 4*G–L*). Together, these findings indicate that liver-specific overexpression of human OATP1B3 protein disturbed the adaptive response of genes to cholestasis involved in BA synthesis, metabolism, and transport, including *Cyp7a1, Cyp3a11*, *Mrp2, Mrp3, Mdr1a, Ostα/β,* and *Ntcp.*

Hepatic Expression of OATP1B3 is Significantly Downregulated in Patients With OC

Next, we examined the expression of hepatic OATP1B3 in patients with OC and control patients. As shown in Figure 5*A–B*, compared with that in the control subjects, the relative levels of hepatic OATP1B3 mRNA transcripts and protein expression were

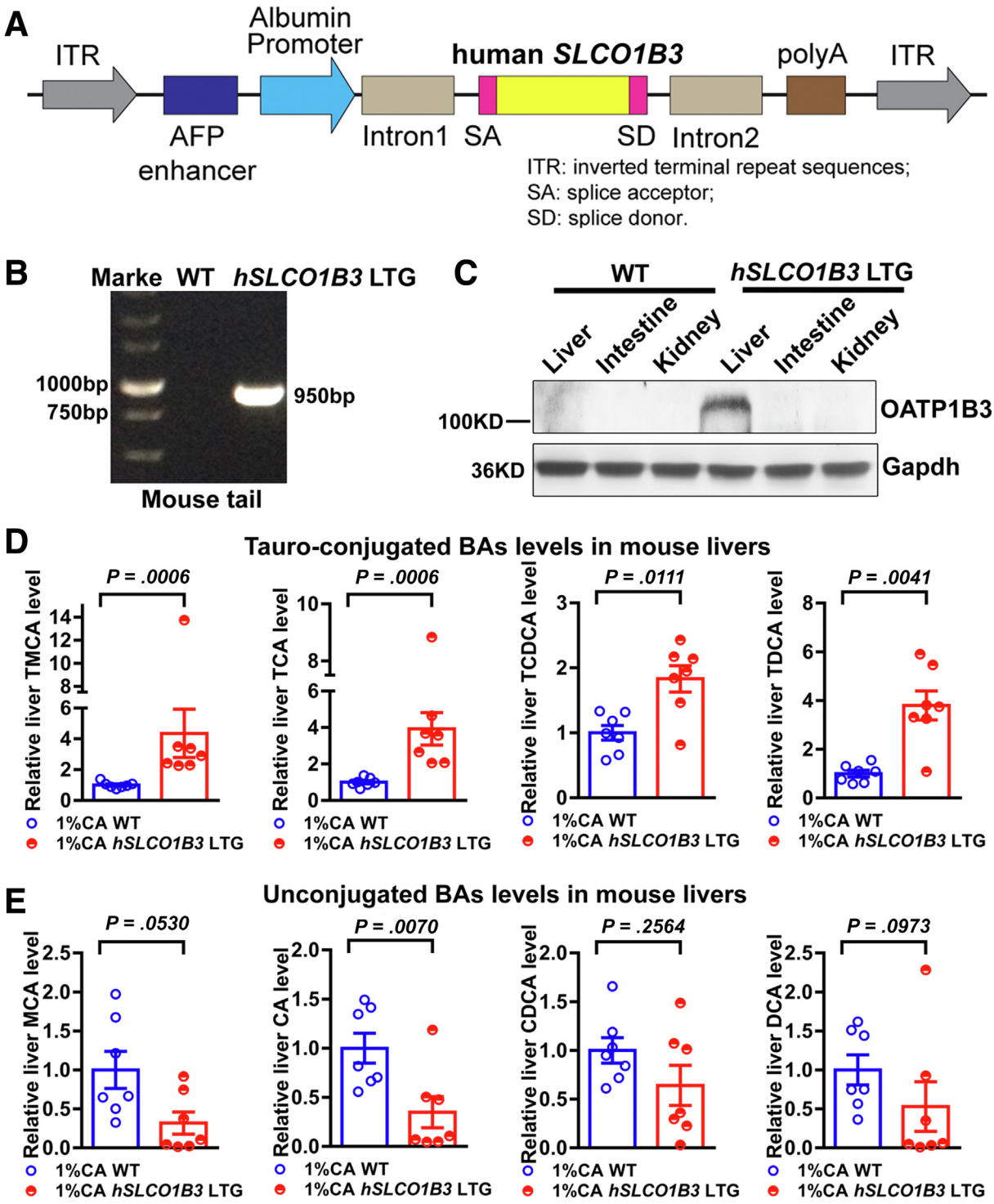

Figure 2. Generation and characterization of *hSLCO1B3* LTG. (*A*) A schematic diagram of the *hSLCO1B3* LTG construct. (*B*) Genotyping of *hSLCO1B3* LTG mice. Genomic DNA was extracted from mouse tails and analyzed by PCR, followed by agarose electrophoresis. (*C*) Western blot analysis of the distribution of OATP1B3 protein expression in *hSLCO1B3* LTG mice. (*D*) HPLC/MS analysis of conjugated BA and (*E*) unconjugated BA levels in liver tissues from WT and *hSLCO1B3* LTG mice after feeding them with 1% CA for 14 days (n = 7 for each group). *hSLCO1B3* LTG, human *SLCO1B3* liver-specific transgenic mice.

dramatically reduced in patients with OC, consistent with reports in other types of cholestasis.[13,14] These data, together with the data from cholestatic transgenic mice, suggest that hepatic OATP1B3 downregulation may be an adaptive protective response against liver injury in human cholestasis.

Table 3. Serum Biochemistry and Total Liver Bile Salt of 8-week-old Mice With 1% CA Diet for 14 Days

	Chow diet, 14 days		1% CA diet, 14 days	
Liver function tests	WT (n = 5)	*hSLCO1B3* LTG (n = 5)	WT (n = 7)	*hSLCO1B3* LTG (n = 7)
ALT, *IU/L*	21.33 ± 1.63	28.34 ± 1.67[a]	183.33 ± 76.66[a,b]	451.67 ± 145.52[a,b,c]
AST, *IU/L*	98.0 ± 5.81	117.50 ± 8.62[a]	189.05 ± 39.67[a,b]	623.76 ± 291.21[a,b,c]
ALP, *IU/L*	142.0 ± 14.08	112.66 ± 30.87	182.38 ± 24.28[a,b]	230.95 ± 59.89[a,b]
TBA, *μmol/L*	5.49 ± 1.17	2.47 ± 1.24[a]	122.01 ± 73.79[a,b]	164.37 ± 202.10
Total liver bile salt, *μmol/kg of liver*	NA	NA	210.63 ± 36.93	400.87 ± 151.31[c]

Note: Data are presented as mean ± standard error of the mean.
ALP, Alkaline phosphatase; ALT, alanine aminotransferase; AST, aspartate aminotransferase; CA, cholic acid; *hSLCO1B3* LTG mice; human *SLCO1B3* liver-specific transgenic mice; NA, not applicable; TBA, total bile salts; WT, wild-type.
[a]$P < .05$ vs WT mice with chow diet.
[b]$P < .05$ vs *hSLCO1B3* LTG mice with chow diet.
[c]$P < .05$ vs WT mice with 1% CA diet.

Proinflammatory Cytokines Such as IL-6, but not BAs, Decreases the Expression of OATP1B3 in Human Hepatoma PLC/RPF/5 Cell Line

To investigate the mechanism of the downregulation of hepatic OATP1B3 in human cholestasis, we tested the effects of BAs and inflammatory cytokines as these chemicals are elevated in cholestatic livers. As shown in (Figure 5*C*), the levels of serum IL-6, IL-8, IL-1β, and TNFα were significantly elevated in patients with OC compared with the controls, implying that elevated serum BAs or proinflammatory cytokines may be associated with hepatic OATP1B3 downregulation in human cholestasis. However, treatment of PLC/RPF/5-*ASBT* cells with conjugated BAs, including GCA, TCDCA, GCDCA, and TDCA, did not decrease *SLCO1B3* mRNA expression in these cells (Figure 5*D*). In contrast, treatment with IL-6 dramatically decreased the levels of *SLCO1B3* mRNA transcripts. Other cytokines including TNFα, IL-8, IL-1β, or CCL2 only moderately reduced *SLCO1B3* mRNA transcripts in the hepatoma PLC/RPF/5 cells (Figure 5*D*), consistent with a previous report in human primary hepatocytes.[18] Furthermore, IL-6 also decreased OATP1B3 mRNA and protein levels in PLC/RPF/5 cells in a dose-dependent manner (Figure 5*E*–*F*). These findings suggest that it is the elevated proinflammatory cytokines, such as IL-6, but not the accumulated conjugated BAs, that directly down-regulate hepatic OATP1B3 expression in human cholestasis.

IL-6/STAT3 Signaling Transcriptionally Represses OATP1B3 Expression in Human Hepatocytes

IL-6, through its receptors, can activate the JAK/STAT3 signaling.[19] Interestingly, the levels of hepatic STAT3 phosphorylation were significantly higher in patients with OC than that in control patients (Figure 6*A*). Therefore, we next investigated whether IL-6 activated STAT3 in human hepatocytes. As shown in (Figure 6*B*–*C*), treatment with different doses of IL-6 did not alter the relative levels of

Table 4. The Levels of Serum Biochemistry and Total Liver Bile Salt in 8-week-old Mice After BDL for 3 Days

	Sham operation, 3 days		BDL operation, 3 days	
Liver function tests	WT (n = 5)	*hSLCO1B3* LTG (n = 5)	WT (n = 8)	*hSLCO1B3* LTG (n = 9)
ALT, *IU/L*	26.67 ± 3.25	20.00 ± 1.71[a]	309.83 ± 44.21[a,b]	542.38 ± 125.20 [a,b,c]
AST, *IU/L*	81.10 ± 3.80	88.52 ± 11.90	476.86 ± 82.88[a,b]	1782.59 ± 421.16[a,b,c]
ALP, *IU/L*	118.34 ± 11.19	82.22 ± 15.03[a]	388.75 ± 59.66[a,b]	595.56 ± 96.57[a,b,c]
TBA, *μmol/L*	1.62 ± 0.08	2.25 ± 1.05	167.69 ± 37.64[a,b]	571.28 ± 141.14[a,b,c]
Total liver bile salt, *μmol/kg of liver*	NA	NA	342.19 ± 81.29[a,b]	770.64 ± 371.78[a,b,c]

Note: Data are presented as mean ± standard error of the mean.
ALP, alkaline phosphatase; ALT, alanine aminotransferase; AST, aspartate aminotransferase; BDL, bile duct-ligation; *hSLCO1B3* LTG; human *SLCO1B3* liver-specific transgenic mice; NA, not applicable. Sham, sham operation; TBA, total bile salts; WT, wild type.
[a]$P < .05$ vs sham WT mice.
[b]$P < .05$ vs sham *hSLCO1B3* LTG mice.
[c]$P < .05$ vs BDL WT mice.

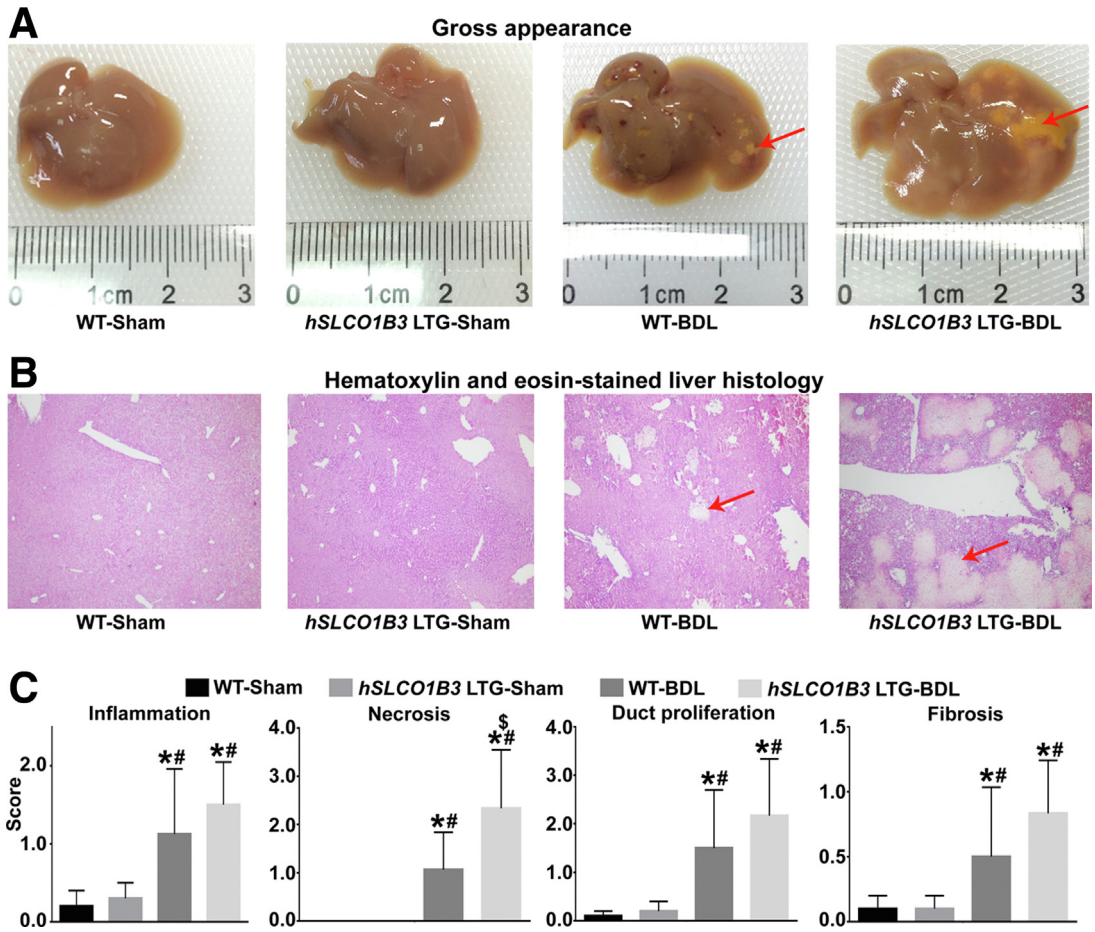

Figure 3. Human OATP1B3 liver-specific overexpression aggravates cholestatic liver injury in BDL mice. (*A*) Representative gross appearance of the liver. (*B*) Hematoxylin and eosin staining of liver morphology. (*C*) Liver histologic assessments, including scores for inflammation, necrosis, fibrosis, and bile-duct proliferation. The histologic assessments were blinded and assessed by expert pathologists. BDL, Mice receiving bile duct-ligation; *hSLCO1B3* LTG, human *SLCO1B3* liver-specific transgenic mice; Sham, mice receiving a sham operation; WT, wild-type mice. *$P < .05$ vs the Sham-WT group; #$P < .05$ vs the Sham-*hSLCO1B3* LTG group; \$$P < .05$ vs the BDL-WT group (n = 5–9 per group).

STAT3 protein expression, but induced STAT3 phosphorylation and increased STAT3 protein in the nucleus in a dose-dependent manner in hepatoma PLC/RPF/5 cells.

To explore how the IL-6/STAT3 signaling reduced OATP1B3 expression in human cholestasis, we analyzed the promoter region of *SLCO1B3* and identified 3 putative STAT3 response elements (Figure 7*A*). Accordingly, 3 luciferase reporter plasmids (pGL3-vector) containing different lengths of the *SLCO1B3* promoter region (−1967 or −261 to +25) were constructed (Figure 7*B*), and co-transfected with the *STAT3 o/e* construct into PLC/RPF/5 cells, followed by treatment with, or without, IL-6. Dual-luciferase reporter assays indicated that treatment with IL-6 or *STAT3 o/e* alone inhibited the *SLCO1B3* promoter activity in PLC/RPF/5 cells, whereas the combination of IL-6 and *STAT3 o/e* further enhanced this inhibition (Figure 6*D*). Interestingly, there were no differences in inhibition of IL-6 and/or *STAT3 o/e* on the activities of 2 truncated forms of the *SLCO1B3* promoter (pGL3-1967/+25 and pGL3-261/+25) in our experimental system (Figure 6*D*), indicating that 2 STAT3 response elements located at −261 to +25 contributed to its promoter activity. Chromatin immunoprecipitation (ChIP) and real-time quantitative polymerase chain reaction (RT-qPCR) assays further confirmed that IL-6 increased the binding activity of STAT3 to the *SLCO1B3* promoter (ChIP site 2: −215 to −205), but not to 2 other elements tested in PLC/RPF/5 cells in a dose-dependent manner (Figure 6*E*). Furthermore, treatment with IL-6 and/or *STAT3 o/e* had no effect on the activity of the pGL3-*SLCO1B3* 261MUT promoter harboring mutations in the key motif of the STAT3 response element in PLC/RPF/5 cells (Figures 7*C*, 6*F*). These findings indicated that the response element located −215 to −205 in the *SLCO1B3* promoter were most critical for downregulating OATP1B3 expression via the IL-6/STAT3 signaling pathway in human hepatocytes.

Moreover, ChIP assays demonstrated that treatment with APTSTAT3-9R, a specific STAT3 binding peptide that inhibits STAT3 activation, completely abrogated the IL-6-induced binding activity of STAT3 to the *SLCO1B3* promoter (ChIP site 2: −215 to −205) in PLC/RPF/5 cells (Figure 6*G*). Additionally, ChIP assays in human livers also demonstrated increased STAT3 binding to the *SLCO1B3* promoter (ChIP site 2: −215 to −205) in patients with OC

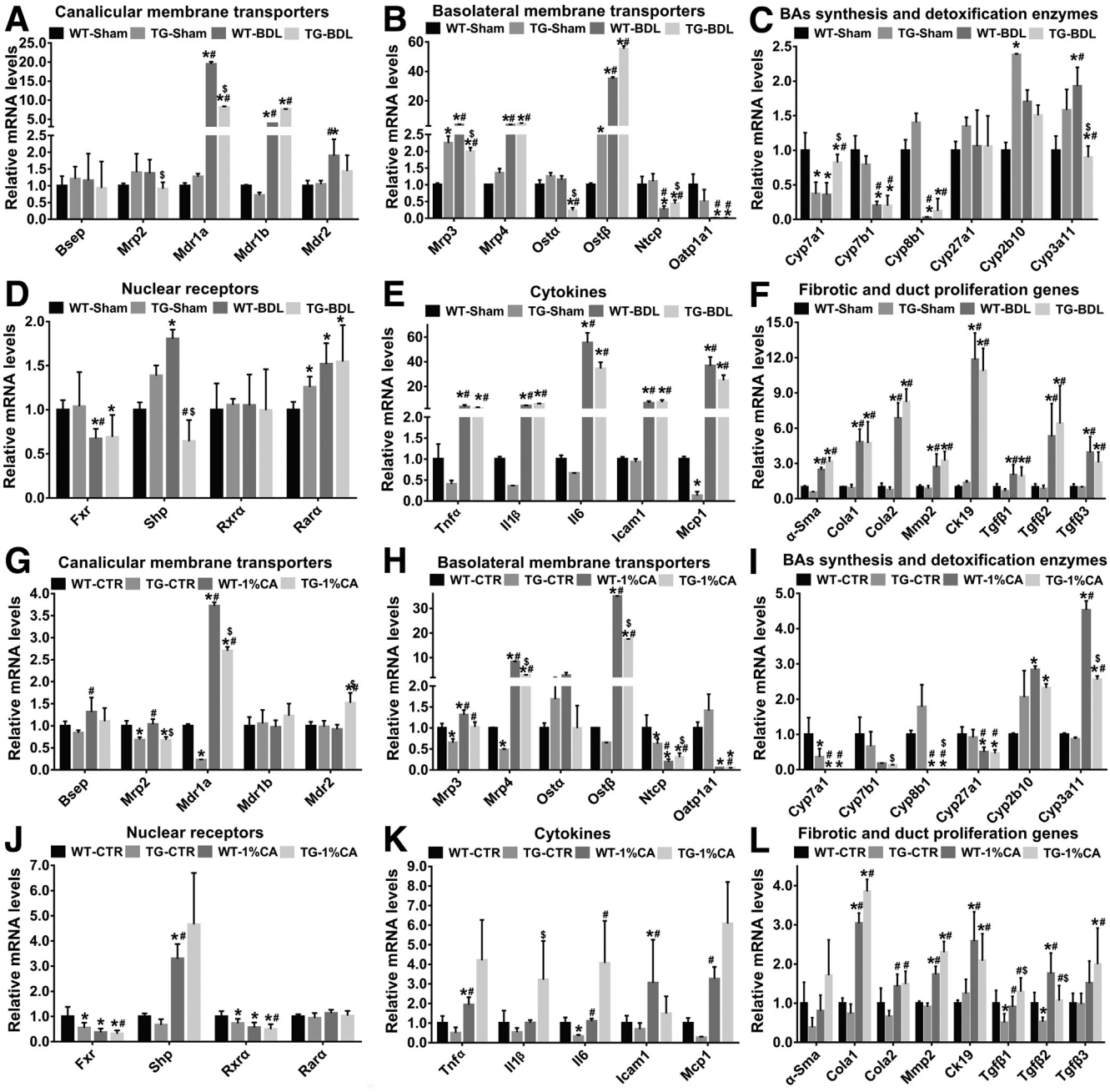

Figure 4. Human OATP1B3 liver-specific overexpression disturbs hepatic expression of genes for the adaptive response to cholestasis in BDL mice or 1% CA-fed mice for 14 days. The livers in BDL or 1% CA-fed mice were sampled and the relative levels of gene mRNA transcript in individual liver samples were quantitatively analyzed by RT-qPCR. The relative levels of liver mRNA transcripts of (*A, G*) canalicular membrane transporters of *Bsep, Mrp2, Mdr1a, Mdr1b,* and *Mdr2*; (*B, H*) basolateral membrane transporters of *Mrp3, Mrp4, Ostα/β, Ntcp,* and *Oatp1a1*; (*C, I*) BA synthesis and detoxification enzymes of *Cyp7a1, Cyp7b1, Cyp8b1, Cyp27a1, Cyp2b10,* and *Cyp3a11*; (*D, J*) nuclear receptors of *Fxr, Shp, Rxrα,* and *Rarα*; (*E, K*) cytokines of *Tnfα, Il1β, Il6, Icam1,* and *Mcp1*; and (*F, L*) fibrotic and bile duct cell proliferation genes of *α-Sma, Cola1, Col1a2, Mmp2, Mmp9, Ck19, Tgfβ1, Tgfβ2,* and *Tgfβ3.* (The value in the WT sham group was designated as 1). TG-BDL, human *SLCO1B3* liver-specific transgenic mice with bile duct-ligation; TG-1% CA, human *SLCO1B3* liver-specific transgenic mice fed with 1% CA diet group; TG-CTR, human *SLCO1B3* liver-specific transgenic mice with control diet group; TG-Sham, human *SLCO1B3* liver-specific transgenic mice receiving sham procedure; WT-BDL, wild-type bile duct-ligation group; WT-1% CA, wild-type mice fed with 1% CA diet group; WT-CTR, Wild-type control diet group; WT-Sham, wild-type sham group. $^*P < .05$ vs the WT sham or control diet group; $\#P < .05$ vs the *hSLCO1B3* LTG sham group; $\$P < .05$ vs the WT-BDL or 1% CA diet group. (n = 3–8 per group).

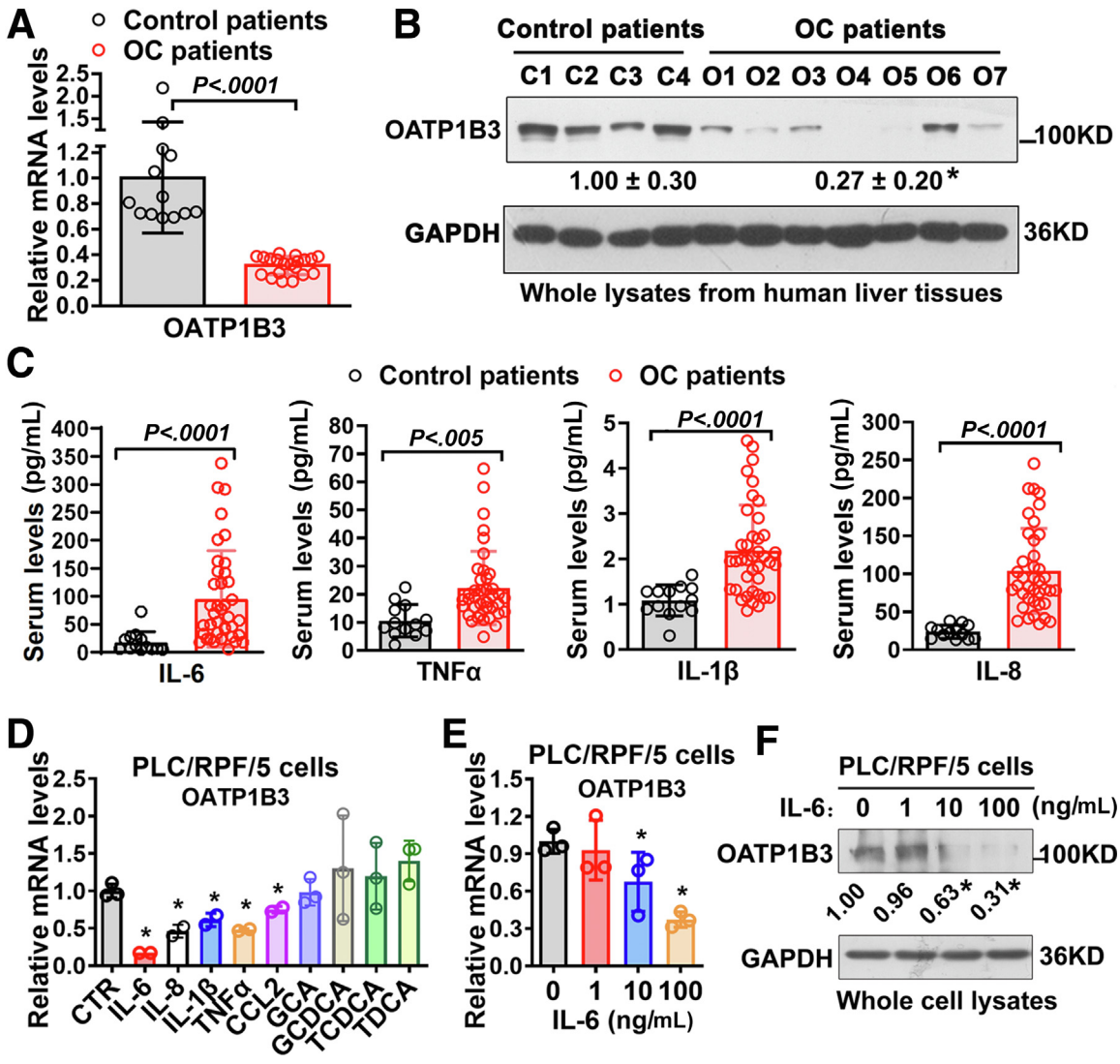

Figure 5. Hepatic OATP1B3 downregulation is associated with increased levels of serum proinflammatory cytokine IL-6 in patients with OC. (*A*) RT-qPCR analysis of the relative levels of *SLCO1B3* mRNA transcripts in control (n = 13) and patients with OC (n = 20). (*B*) Representative Western blots of hepatic OATP1B3 protein expression. *C:* controls; *OC:* obstructive cholestasis. *$P < .05$ vs the controls. (*C*) The levels of serum IL-6, IL-1β, TNFα, and IL-8 in patients with OC (n = 39) and controls (n = 13). (*D*) The levels of *SLCO1B3* mRNA transcripts in PLC/RPF/5 cells after treatment with cytokines (100 ng/mL) or BAs (100 μM). *$P < .05$ vs CTR (control). (*E*) IL-6 reduced *SLCO1B3* mRNA expression in a dose-dependent manner in PLC/RPF/5 cells. *$P < .05$ vs control (0 ng/mL). (*F*) Treatment with IL-6 also reduced OATP1B3 protein expression in PLC/RPF/5 cells in a dose-dependent manner. n = 3; *$P < .05$ vs control (0 ng/mL).

compared with controls (Figure 6*H*), along with elevated levels of serum IL-6 (Figure 5*C*). Altogether, these data indicate that activation of IL-6/STAT3 signaling repressed hepatic OATP1B3 expression in human cholestasis.

Conjugated BAs Induce Cxcl2 and Ccl2 Expression in WT and Slc10a1^{hSLCO1B3} Hepatocytes but not in Slc10a1$^{-/-}$ Hepatocytes to Attract Neutrophil Infiltration, Leading to IL-6 Production

Finally, whether and how intrahepatic conjugated BAs stimulated the production of serum inflammatory cytokines such as IL-6 in cholestasis was investigated in vitro. Primary neutrophils prepared from WT mice and primary hepatocytes isolated from WT, *Slc10a1*$^{-/-}$ or *Slc10a1*^{hSLCO1B3} mice were co-cultured in transwell plates, followed by stimulation of hepatocytes with conjugated BA (Figure 8*A*). As shown in (Figure 8*B*–*C*), GCA stimulation significantly increased the numbers of migrated neutrophils across the transwell membrane in co-cultured primary WT or *Slc10a1*^{hSLCO1B3} hepatocyte groups, but not in co-cultured *Slc10a1*$^{-/-}$ hepatocyte groups. Furthermore, glycocholate acid (GCA) stimulation also significantly increased the relative levels of *Ccl2* and *Cxcl2* mRNA transcripts in co-cultured WT and *Slc10a1*^{hSLCO1B3} primary hepatocytes, but not in co-cultured *Slc10a1*$^{-/-}$ primary hepatocytes

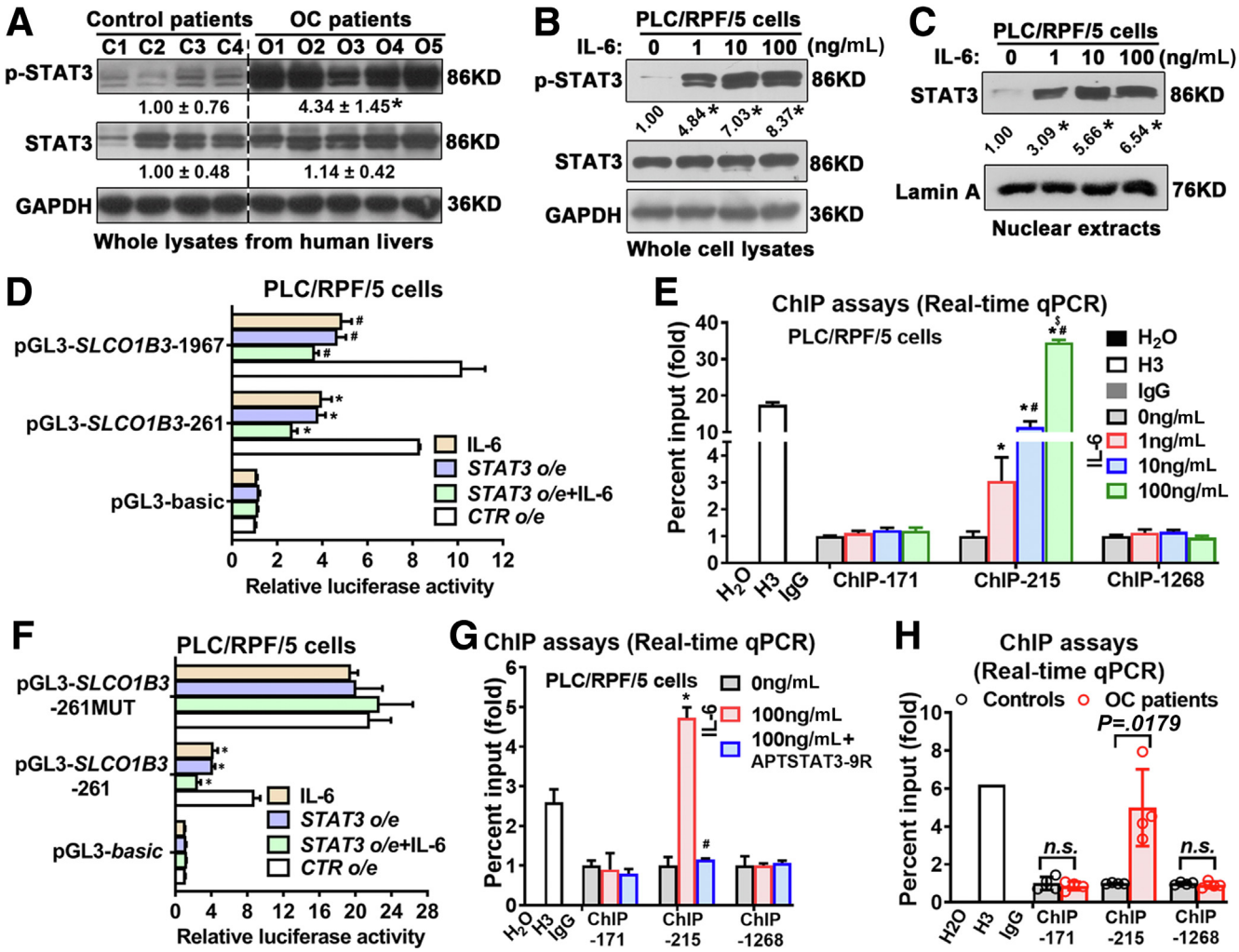

Figure 6. The activation of IL-6/STAT3 signaling transcriptionally downregulates OATP1B1 expression in hepatocytes. (*A*) Western blot analysis of the relative levels of hepatic STAT3 expression and phosphorylation in patients with OC (n = 20) and control patients (n = 13). *$P < .05$ vs controls. (*B*) IL-6 induced STAT3 phosphorylation and (*C*) nuclear STAT3 protein expression in PLC/RPF/5 cells in a dose-dependent manner. n = 3; *$P < .05$ vs control (0 ng/mL). (*D*) Dual luciferase reporter assays revealed that treatment with IL-6 and *STAT3 o/e* attenuated the *SLCO1B3* promoter activity (pGL3-*SLCO1B3*-1967 or pGL3-*SLCO1B3*-261) in PLC/RPF/5 cells in vitro. PLC/PRF/5 cells were transiently transfected with the plasmid for Renilla luciferase expression and control pGL3-basic or plasmid for the pGL3-*SLCO1B3*-1967 or pGL3-*SLCO1B3*-261, together with control plasmid (*CTR* o/e) or the plasmid for STAT3 overexpression (*STAT3 o/e*). One day later, the cells were treated with, or without, 100 ng/mL IL-6 for 12 hours. The luciferase activity of each group of cells was quantified by dual-luciferase reporter assays. *$P < .05$ or #$P < .05$ vs *CTR o/e*. (*E*) ChIP assays (RT-qPCR method) indicated that IL-6-activated STAT3 bound to the *SLCO1B3* promoter (ChIP 2 site: −215 to −205) in PLC/PRF/5 cells in a dose-dependent manner. *$P < .05$ vs the 0 ng/mL IL-6 group; #$P < .05$ *vs.* the 1 ng/mL IL-6 group; $$P < .05$ vs the 10 ng/mL IL-6 group. (*F*) Treatment with IL-6 and/or *STAT3 o/e* inhibited the pGL3-*SLCO1B3*-261 promoter activity, but not its mutant promoter activity (pGL3-*SLCO1B3*-261MUT) in PLC/RPF/5 cells. *$P < .05$ vs the *CTR o/e*. (*G*) ChIP assays (RT-qPCR method) unveiled that treatment with APTSTAT3-9R, a specific STAT3-binding peptide, abrogated the increased activity of IL-6-activated STAT3 binding to the *SLCO1B3* promoter (ChIP 2 site: −215 to −205) in PLC/RPF/5 cells. *$P < .05$ vs the 0 ng/mL group; #$P < .05$ vs the 100 ng/mL group. (*H*) ChIP assays (RT-qPCR method) revealed that there were more activated STAT3 bound to the *SLCO1B3* promoter in the liver of patients with OC than control patients.

(Figure 8*D*). The similar levels of *Ccl2* and *Cxcl2* mRNA transcripts induced by GCA in co-cultured WT or *Slc10a1*^{hSLCO1B3} primary hepatocytes also confirm that in comparison with mouse Ntcp, human OATP1B3 may have a similar capacity to take up conjugated BAs in mice. In addition, previous studies reported that conjugated BAs stimulate EGR1 expression in cholestatic mouse livers and the activation of EGR1 induces the expression of Ccl2 and Cxcl2 in hepatocytes.[24,25] As shown in (Figure 8*E*), hepatic EGR1 protein levels were significantly increased in patients with OC compared with their controls. Thus, these findings support the concept that the accumulated BAs induce Ccl2

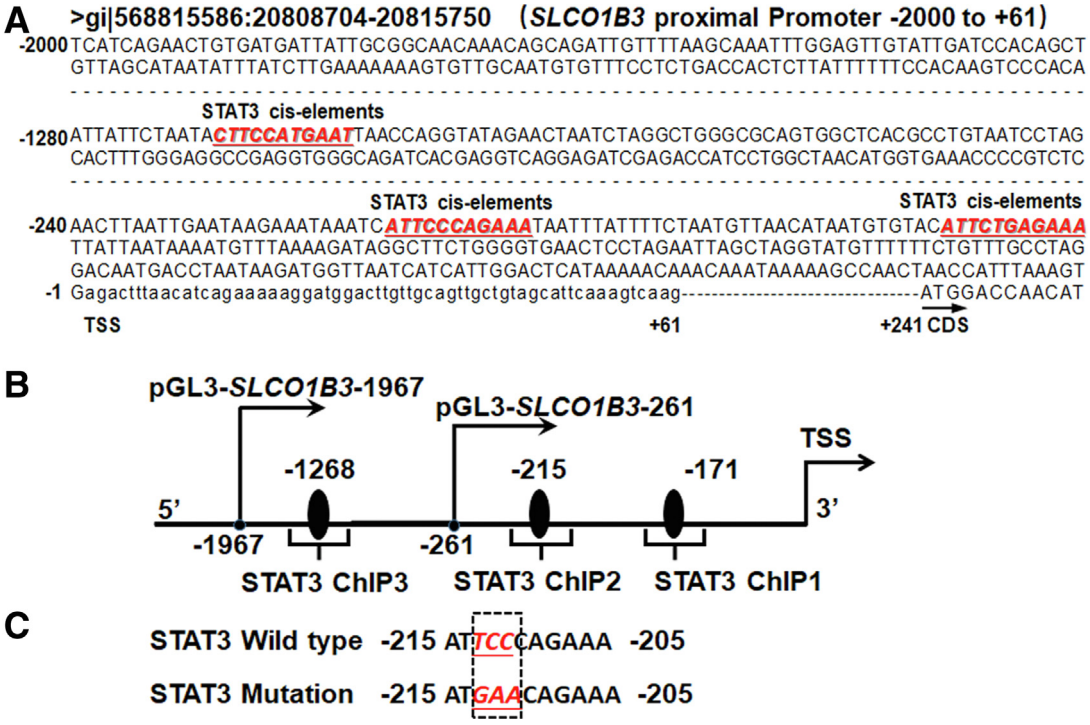

Figure 7. Analysis of the *SLCO1B3* promoter. (*A*) Putative STAT3 cis-elements were identified in the proximal promoter region of the human *SLCO1B3* gene (http://jaspar.genereg.net). (*B*) A diagram for illustration of ChIP and luciferase reporter assays of the human *SLCO1B3* promoter. (*C*) The key motif mutation of STAT3 potential response elements in the pGL3-*SLCO1B3*-261 construct.

and Cxcl2 production in hepatocytes where the activation of EGR1 is involved, which attracts neutrophils to produce IL-6 in the liver, and that this process depends on the function of 2 key BA uptake transporters, OATP1B3 and NTCP.

Discussion

In the current study, we examined the functional significance of hepatic OATP1B3 for the normal physiologic process of hepatic bile acid uptake as well as its adaptive response in cholestasis. To do so, we created 3 genetic mouse models (ie, *Slc10a1*$^{-/-}$, *Slc10a1*^{hSLCO1B3}, and *hSLCO1B3*-LTG). Knockin of *hSLCO1B3* driven by endogenous mouse *Slc10a1* promoter in a *Slc10a1*$^{-/-}$ background provided a cleaner system, excluding the influence of Ntcp to assess OATP1B3 substrate specificity for BA. The creation of *hSLCO1B3*-LTG mice where hepatic OATP1B3 was constitutively expressed further allows us to address the significance of its regulated expression in cholestasis. Using these genetic models, we made the following major findings: (1) OATP1B3 is an important bile acid transporter for the in vivo uptake of BA in the liver and can partially compensate the function of Ntcp for hepatic uptake of conjugated BAs in mice (Figure 1; Table 1); (2) Human OATP1B3 liver-specific overexpression significantly increased intrahepatic BA accumulation and aggravated liver injury in cholestatic mice (Figures 2–3 and Tables 3–4); and (3) Hepatic OATP1B3 expression was transcriptionally downregulated in patients with OC, which was mediated through the IL6/STAT3 signaling pathway (Figures 6–8). These novel findings highlight the significant role that the OATP1B3 transporter plays for BA uptake in the liver, whereas its downregulation during cholestasis provides for an adaptive protective response.

Hepatic OATP transporters are crucial for the hepatic clearance of both endogenous compounds and xenobiotics from the systemic circulation.[3-8] Their functions are distinct in some circumstances. For example, hepatic OATP3A1 is a BA efflux transporter, and its expression is markedly upregulated in human cholestasis to reduce excessive intrahepatic BAs.[23] In contrast, hepatic OATP1B3 is thought to be an uptake transporter for a broad range of substrates, including BAs.[4-8] Its expression is downregulated in patients with OC (Figure 5) as demonstrated in this study and reported in several other cholestatic diseases (eg, PBC, PFIC-2 and -3, and ICP).[13,14] Decreased OATP1B3 expression has been thought to protect the liver from cholestatic injury by reducing hepatic BA uptake.[1,2] However, there was no experimental evidence to support this concept. In addition, how hepatic OATP1B3 expression is downregulated in cholestasis remains poorly understood. The current study is the first to report that human OATP1B3 liver-specific overexpression significantly increases intrahepatic BA accumulation and aggravates cholestatic liver injury in mice (Figures 2–3 and Tables 3–4). It is well known that the accumulated BAs trigger hepatic inflammatory response and initiate cholestatic liver injury.[15] Interestingly, higher levels of serum proinflammatory cytokines such as IL-6 were also

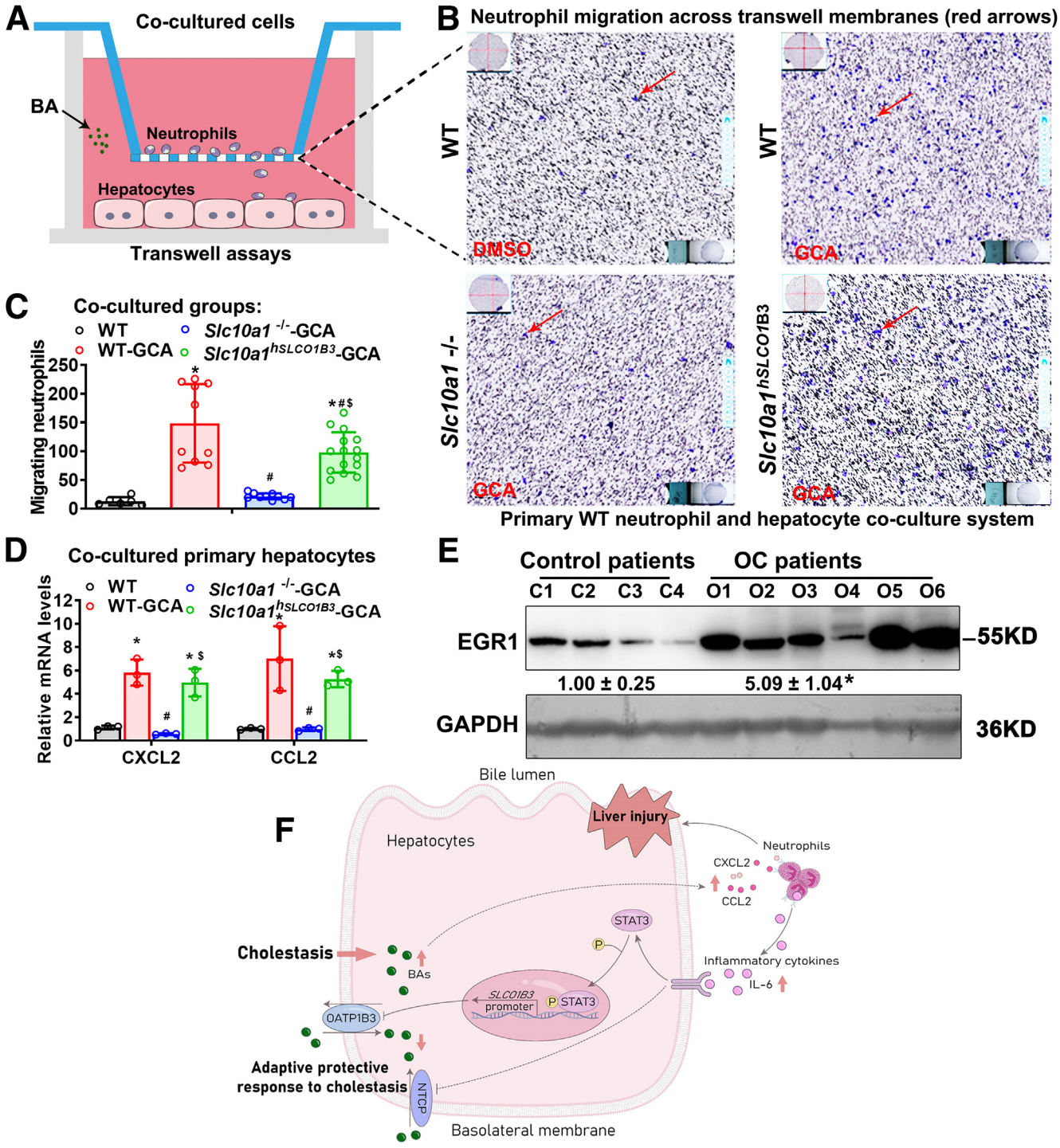

Figure 8. Conjugated BAs stimulate Ccl2 and Cxcl2 production in WT and *Slc10a1*^{hSLCO1B3} hepatocytes, but not in *Slc10a1*$^{-/-}$ hepatocytes to attract neutrophil migration, producing IL-6 in a co-culture system. (*A*) A diagram for illustration of the co-culture system in transwell plates. (*B*) and (*C*) Examinations of migration ability of co-cultured WT neutrophils across the transwell membrane after co-cultured with the primary hepatocytes from WT, *Slc10a1*$^{-/-}$ or *Slc10a1*^{hSLCO1B3} *mice* in the presence or absence of 100 μM GCA. (*D*) RT-qPCR analysis of the relative levels of *Cxcl2* and *Cxl2* mRNA transcripts in co-cultured WT, *Slc10a1*$^{-/-}$ or *Slc10a1*^{hSLCO1B3} primary hepatocytes. *$P < .05$ vs WT primary hepatocyte group; #$P < .05$ vs WT primary hepatocyte-GCA group; \$$P < .05$ vs *Slc10a1*$^{-/-}$ primary hepatocyte-GCA group. (*E*) Representative Western blots of hepatic EGR1 protein expression. C: controls. *$P < .05$ vs controls. (*F*) A schematic diagram for illustration of a novel negative feedback mechanism against cholestasis.

detected in patients with OC (Figure 5*C*). Furthermore, previous studies reported that BA stimulated IL-6 production in cholestatic-associated liver injury.[26] Based on these findings, we propose a new regulatory mechanism for hepatic OATP1B3 downregulation in human cholestasis (Figure 8*F*): First, accumulated intrahepatic BAs stimulate the production of chemokines (eg, Ccl2 and Cxcl2) in hepatocytes to attract neutrophils and other inflammatory cell infiltrates in the liver where the activation of hepatic EGR1 is involved.[15,24,25] These activated neutrophils and other inflammatory infiltrates produce high levels of proinflammatory cytokines, such as IL-6. IL-6 then activates the JAK/STAT3 signaling pathway through its receptors IL-6R/gp130 to repress hepatic OATP1B3 expression by increasing STAT3 binding to the *SLCO1B3* promoter. Finally, the reduced expression of hepatic OATP1B3 impairs uptake of conjugated BAs from blood into hepatocytes. Consequently, this negative feedback mechanism serves to attenuate BA-induced cholestatic liver injury (Figure 8*F*).

NTCP/*SLC10A1* is a key BA uptake transporter on the basolateral membrane of hepatocytes,[1-3] and its deficiency leads to a remarkable elevation of serum BAs in mice.[10] Similarly, OATP1B3 transports conjugated BAs with a high affinity in vitro, suggesting that it may also be a significant BA transporter in physiological conditions.[6] However, in comparison with NTCP, the functional significance of OATP1B3 for BA uptake in physiological and cholestatic conditions has been unclear. The current study first discovered that human OATP1B3 liver-specific overexpression markedly increased intrahepatic accumulation of conjugated BAs, but not unconjugated BAs, in mice following feeding with 1% CA (Figure 2), suggesting that OATP1B3 may directly contribute to conjugated BA accumulation in liver tissues by transporting them from blood to hepatocytes. We also observed a remarkable elevation in the levels of serum TBA in *Slc10a1*$^{-/-}$ mice, consistent with a previous report.[10] Strikingly, this dramatic increase in the levels of serum BAs induced by Ntcp deficiency was completely diminished in *Slc10a1*^{hSLCO1B3} mice, even after feeding with 0.1% UDCA to challenge hepatic BA uptake (Table 1). Functional studies in the uptake of [^{3}H]-TCA in vitro and TCA-induced bile flow in vivo further confirmed that in comparison to Ntcp, hepatic OATP1B3 has a similar ability to take up conjugated BAs (Figure 1*F–G*), although it does not seem to completely compensate the function of Ntcp in mice. Therefore, our findings provided evidence that OATP1B3 functions as a significant transporter for the hepatic uptake of conjugated BAs and can partially compensate Ntcp for BA uptake in mice.

Currently, there are no clinical reports of patients with OATP1B3 mutations. However, both *SLCO1B3* and *SLCO1B1* deficiency leads to the Rotor syndrome with a high level of serum bilirubin,[9] highlighting the importance of both OATPs in uptake of bilirubin in the liver. Because human OATP1B3 is poorly conserved among species without mouse orthologs, Ntcp deficiency alone causes a dramatic elevation in the levels of serum BAs in mice (Table 1).[10] In contrast, OATP1B3 and NTCP share this function in humans so that if one has a loss-of-function, its BA uptake function can be compensated by the other. This may explain why loss-of-function mutations in *SLCO1B3* do not increase serum BA levels in human subjects.[9] To date, few cases carried with homozygous mutation (p.R252H) in NTCP/*SLC10A1* exhibited conjugated hypercholanemia.[11,12] However, the levels of serum BAs in these patients are highly variable but often excessively high.[11,12] It may be attributed to the loss function of NTCP, because hepatic OATP1B3 can partially compensate its function for conjugated BA uptake (Figure 1*F–G*) and hepatic OATP1B3 protein expression levels were significant heterogeneity in human control livers (Figure 5*B*). In addition, recent studies have described some patients with hypercholesterolemia that carry a homozygous p.S267F mutation in *SLC10A1*.[27] However, we did not observe any abnormal levels of serum BAs in *Slc10a1*^{S267F} homozygous mice,[28] even after challenging them with 0.1% UDCA (Table 5). Future studies should test whether these patients might carry mutations in *SLCO1B3* or other BA efflux transporters, such as *OST*α/β, to understand the molecular mechanisms underlying these phenomena.

In summary, this study is the first report that OATP1B3 functions as a significant transporter for hepatic BA uptake and can partially compensate Ntcp for conjugated BA uptake in mice and in primary hepatocytes. Human OATP1B3 liver-specific overexpression increased hepatic conjugated BA accumulation and cholestatic liver injury in mice with 1% CA-fed-induced cholestasis. Therefore, downregulation of hepatic OATP1B3 is an adaptive protective response against cholestasis in humans.

Materials and Methods

Generation and Validation of *Slc10a1*$^{-/-}$ Mice

The *Slc10a1*$^{-/-}$ mice were designed and generated by Shanghai Model Organisms Center (Shanghai, China). Briefly, Cas9 mRNA was transcribed in vitro with the mMESSAGE mMACHINE T7 Ultra Kit (Ambion), according to the manufacturer's instructions (Figure 1*A*). Two specific guide RNAs (sgRNAs) targeting *Slc10a1* exons 2–4 were in vitro transcribed using the MEGAshortscript T7 Transcription Kit (ThermoFisher). One sgRNA targeting *Slc10a1* intron 1 was 5'-GGGATCAAATCCACCATAAAGGG-3'; another sgRNA targeting *Slc10a1* intron 2 was 5'-TAGACGATGTGGTGGTAGCTCGG-3'. To generate *Slc10a1*$^{-/-}$ mice, zygotes were isolated from C57BL/6 mice and injected with the in vitro-transcribed Cas9 mRNA and sgRNAs, followed by transferring into pseudo-pregnant C57BL/6 recipients. The obtained F0 mice were characterized by PCR and sequencing using specific primers F-5'-TTATCGCTATGACTTTCTACCTGT-3'; R-5'-GCTATTGG-GATCTT ATTTCTCTTG-3'. The positive F0 male mice were bred with WT female C57BL/6 mice to obtain F1 heterozygous *Slc10a1*$^{+/-}$ mice. The genotype of F1 mice was identified by PCR and confirmed by sequencing (Figure 1*B*). Male and female F1 heterozygous *Slc10a1*$^{+/-}$ mice were bred to produce the homozygous *Slc10a1*$^{-/-}$ C57BL/6 mice.

Generation and Identification of *Slc10a1*^{hSLCO1B3} Mice

The *Slc10a1*$^{hSLCO1B3/hSLCO1B3}$*Slc10a1*$^{-/-}$ homozygous mice (abbreviated as *Slc10a1*^{hSLCO1B3} mice) with both endogenous

Table 5. Serum Biochemistry of *Slc10a1*^{S267F} Mutant Mice (8 weeks old)

	Wild type [28] (n = 4)	Heterozygote [28] (n = 4)	Homozygote [28] (n = 7)	0.1%UDCA-Homozygote (n = 6)
Serum ALT, *IU/L*	22.98 ± 4.36	37.18 ± 9.83	29.95 ± 2.98	28.12 ± 1.79
Serum AST, *IU/L*	76.54 ± 6.67	81.60 ± 10.37	75.15 ± 8.33	79.79 ± 5.06
Serum ALP, *IU/L*	47.36 ± 7.35	34.56 ± 3.05	30.35 ± 3.28	33.71 ± 3.33
Serum TBA, *μmol/L*	2.65 ± 1.82	2.33 ± 0.76	3.06 ± 0.67	3.95 ± 0.25

Note: Data are presented as mean ± standard error of the mean.
Note: Serum data of wild-type, heterozygote, and homozygote groups were described in our previous study.[28]
ALP, Alkaline phosphatase; ALT, alanine aminotransferase; AST, aspartate aminotransferase; TBA, total bile acids; UDCA, ursodeoxycholic acid.

Slc10a1 promoter-driven human *SLCO1B3* expression and *Slc10a1* exon2 knockout were generated by Shanghai Model Organisms Center (Shanghai, China) as follows.

First, the *Slc10a1*$^{+/hSLCO1B3}$ knock-in mice with mouse *Slc10a1* promoter-driven human *SLCO1B3* expression were generated (Figure 1*C*). Briefly, the DNA fragment coding human *SLCO1B3* was linked to the WPRE and polyA sequence, which were flanked with the up- and downstream DNA sequences of the ATG codon of the *Slc10a1* as the recombination donor DNA construct. A Cas9 mRNA was prepared by in vitro transcription using mMESSAGE mMACHINE T7 Ultra Kit (Ambion), according to the manufacturer's instructions, and purified using the MEGAclearTM Kit (ThermoFisher). A sgRNA targeting the 5'-GTGTTCACTGGGTCGGAGGATGG-3' sequence was prepared by in vitro transcription using the MEGAshortscript Kit (ThermoFisher) and purified using the MEGAclearTM Kit. The donor DNA, sgRNA, and Cas9 mRNA were microinjected into fertilized eggs from C57BL/6 mice. Following the process of gene editing and homologous recombination, the potential positive F0 mice were identified by long PCR using specific primers. The sequences of primers P1: 5'-GGCAGACTTCAATAACTTCATACATACA-3' and P2: 5'-CAGACTGGTTCCCACTGACTTTC-3' for the correct 5' homology arm recombination, and P3: 5'-CACTGAGGGGATGAAGCAAAAG-3' and P4: 5'-CCAGGTAGCAAGGGTGACAGG-3' for the correct 3' homology arm recombination. The PCR products were further confirmed by sequencing. Male F0 mice were bred with WT female C57BL/6 mice to obtain *Slc10a1*$^{+/hSLCO1B3}$ heterozygous mice.

Next, to ensure disruption of *Slc10a1* gene expression, exon 2 of *Slc10a1* in *Slc10a1*$^{+/hSLCO1B3}$ heterozygous mice was further deleted using the Crispr/cas9 system and specific sgRNAs that were prepared by in vitro transcription using the MEGAshortscript Kit (ThermoFisher). The targeting sequences of sgRNAs were 5'-GCCACTTACTATGTCCAATCCGG-3' and 5'-ACATTCAACTCTAACCCCTAGGG-3' locating in the intron 1 and 2 of *Slc10a1*, respectively. The prepared Cas9 mRNA and sgRNAs were injected into zygotes of *Slc10a1*$^{+/hSLCO1B3}$ mice and transferred to pseudopregnant mice. The genomic DNAs were isolated from F0 mice and tested by PCR and sequenced using the primers of F-5'-ATAAAGGGGAAGACATGGCAATAG-3'; R-5'-TTTCTGGTCTTCGGTAGTCGTCTT-3'. The positive male F0 mice were bred with C57BL/6 mice to obtain F1 heterozygous mice. The genotype of F1 mice was identified by PCR and confirmed by sequencing (Figure 1*D*). Male and female F1 heterozygous mice were bred to produce the homozygous *Slc10a1*$^{hSLCO1B3/hSLCO1B3}$*Slc10a1*$^{-/-}$ mice (abbreviated as *Slc10a1*^{hSLCO1B3} mice).

Generation and Identification of Human SLCO1B3 Liver-specific Overexpression Transgenic Mice

Liver-specific overexpression of human *SLCO1B3* transgenic (*hSLCO1B3* LTG) mice were generated using the Piggybac transposon system by Shanghai Model Organisms Center (Shanghai, China). Specifically, the full-length DNA fragment for coding *SLCO1B3* was cloned into a pLIVE vector with the minimal albumin promoter and mouse alpha fetoprotein enhancer II (Figure 2*A*). In vitro transcription of capped Piggybac transposase mRNA was generated using the mMESSAGE mMACHINE kit (Ambion), according to the manufacturer's instruction. The transposase mRNA was mixed with circular PB-LIVE-OATP1B3 vector and microinjected into fertilized oocytes from C57BL/6J mice, as described.[29] Transgenic founders were identified by PCR using the primers (F-5'-ACCGGGGACCCAGTAACC-'3; R- 5'-TCCAACCCAACGAGAGTCCTT-'3) with a 950bp PCR product (Figure 2*B*). Finally, the expression levels of OATP1B3 in *hSLCO1B3* LTG mice were confirmed by Western blotting analysis (Figure 2*C*).

Animal Studies

WT C57BL/6J mice were purchased from the Center of Laboratory Animals of Third Military Medical University (Chongqing, China). The animals were housed in our specific pathogen-free facility, and all the mice included in experiments were male. For the 14-day 0.1% UDCA feeding experiment, 8-week-old WT, *Slc10a1*$^{-/-}$, and *Slc10a1*^{hSLCO1B3} mice were randomized and fed with control chow (n = 10 for the WT group; n = 7 for the *Slc10a1*$^{-/-}$ group; and n = 8 for the *Slc10a1*^{hSLCO1B3} group) or with 0.1% UDCA (n = 8 for each genotype). For the 14-day 1% CA feeding experiment, 8-week-old WT and h*SLCO1B3* LTG mice were randomized and fed with control chow (n = 5 for each genotype) and 1% CA diet (n = 7 for each genotype), respectively. For the

3-day BDL experiments, 8-week-old WT and h*SLCO1B3* LTG mice were randomized and subjected to a sham operation (n = 5, for each genotype) and BDL (n = 8 for the WT group, n = 9 for the h*SLCO1B3* LTG group). The animals were fasted overnight. Before euthanasia, their peripheral blood samples were collected for preparation of serum samples, which were immediately stored at −80 °C until analyses. The levels of serum biomarkers in individual mice were assayed by the Section of Clinical Laboratory, Southwest Hospital (Third Military Medical University, Chongqing, China). The liver tissues were dissected from individual mice, washed with cold phosphate buffered saline, and immediately cut into small pieces, followed by rapidly freezing in liquid nitrogen until analysis.

Animal experiments were conducted, according to the guidelines of the Animal Care and Use Committee at the Southwest Hospital affiliated with the Third Military Medical University (Chongqing, China). The experimental protocol was approved by the Institutional Animal Care and Use Committee (Third Military Medical University).

Patients and Liver Samples

OC liver tissues (n = 39) were obtained from patients, who underwent pancreastoduodenectomy procedure for a suspected pancreatic or periampullary malignancy, and the demographic and clinical characteristics of these patients are summarized as described previously.[23] Control liver tissues without cholestasis were also collected from patients undergoing resection of liver metastases (n = 13). The collected liver samples were immediately cut into small pieces and fixed in 4% paraformaldehyde or frozen in liquid nitrogen.

Studies involving human subjects were carried out in accordance with the Declaration of Helsinki (2013) by the World Medical Association and approved by the Institutional Ethical Review Board at Southwest Hospital Affiliated to Army Medical University (Third Military Medical University, Chongqing, China). In the current study, the patients were recruited from the Institute of Hepatobiliary Surgery and the Department of Gastroenterology at Southwest Hospital, Third Military Medical University. All patients signed a written informed consent form prior to the start of this study.

Special Reagents

Special reagents used in the study included dimethyl sulfoxide (DMSO) and various BAs of UDCA, GCA, TCDCA, TMCA, GCDCA, and TDCA (Sigma-Aldrich Chemical); [^{3}H]-TCA (1 mCi/mL, PerkinElmer Life and Analytical Sciences)[23]; human recombinant IL-6, IL-1β, TNFα, and CCL2 (Peprotech); and APTSTAT3-9R (Cat#S8197), an inhibitor of STAT3 phosphorylation (Selleck Chem).

Measurements of [^{3}H]-labeled TCA Uptake in Primary Mouse Hepatocytes

Primary mouse hepatocytes were isolated from 10- and 20-week-old WT, *Slc10a1*$^{-/-}$ or *Slc10a1*^{hSLCO1B3} mice using a collagenase perfusion protocol.[28] The isolated hepatocytes ($\sim 0.8\times10^6$ cells/well) were cultured in 5% fetal bovine serum (FBS)-Williams' Medium E and treated in triplicate with 1 pM [^{3}H]-TCA for 30 minutes. The cells were harvested and washed. Their cell lysates were prepared and the contents of intracellular [^{3}H]-labeled TCA in individual cell lysate samples were measured by the LS analyzer (Beckman instrument, Inc).

Mouse Tail Vein Injection of Conjugated BA TCA and Bile Flow Measurement

Intravenous infusion of BA combined with bile cannulation were performed to measure biliary secretion of BAs in *Slc10a1*$^{-/-}$, *Slc10a1*^{hSLC01B3} and WT (n = 3 per each group), as reported previously.[30] Briefly, the gallbladder was cannulated, bile samples were collected every 10 minutes and continued for up to 120 minutes, then TCA (30 μmol/L) was infused into the tail vein.

LC-MS/MS Analysis of BA Compositions of Mouse Bile Samples

Bile samples (10 μl) collected from *Slc10a1*$^{-/-}$, *Slc10a1*^{hSLC01B3}, and WT mice were subject to LC-MS/MS analysis as described previously,[23] BA analysis was technically supported by Wuhan Metware Biological Technology Co, Ltd.

Neutrophil Isolation

Mouse neutrophils were isolated from the bone marrow, as described.[31] Briefly, the femur bones were dissected from WT mice, and the bone marrow suspension was overlaid on the top of the different Percoll gradient layers (52%, 64%, and 72%). After centrifuged, the neutrophils at the 64% to 72% interface were collected and stained with PE-anti-CD11b, FITC-anti-Ly6G, and APC-anti-CD45-APC antibodies (BD PharMingen). The cells were analyzed by flow cytometry (FACSAria II, BD) using FlowJo software.

Transwell Migration Assays

The neutrophil migration induced by chemokines from the GCA-stimulated primary hepatocytes was determined using Transwell migration assays.[15] Briefly, primary mouse hepatocytes were cultured in the bottom chambers of 6-well Transwell plates (Permeable Supports 24-mm insert, 3.0-μm polycarbonate membrane, Costar) in 2.5 mL of medium in the presence or absence of 100 μM GCA and individual inserters were added with 0.6×10^6 neutrophils, followed by incubating them at 37 °C for 3 hours. Subsequently, the unmigrated cells on the upper surface of the inserter chamber membrane were removed, and the migrated cells on the bottom surface of the upper chamber membrane were fixed with 4% paraformaldehyde and stained with crystal violet, followed by counting them under a microscope. The numbers of migrated neutrophils were normalized to the initial number of cultured hepatocytes.

Table 6. The Sequences of Primers for *the SLCO1B3* Promoters and ChIP Assays

Mutants	Primer pairs	Products, bp
pGL3-*SLCO1B3*-Luc(-1967/+46)	F:5'-CGGCTAGC ACAGCAGATTGTTTTAAGCAAA-3' R:5'-CCCAAGCTTTACAGCAACTGCAACAAGTCC-3'	2013
pGL3- *SLCO1B3*-Luc(-261/+46)	F:5'-CGGCTAGC AGAAGAAAATCTTATGCAAC-3' R:5'-CCCAAGCTTTACAGCAACTGCAACAAGTCC-3'	307
pGL3- *SLCO1B3*-Luc(-261/+46) MUT	F:5'-ATCAT***GAA***CAGAAATAATTTATTTTCTAATGT -3' F:5'-ACATTAGAAAATAAATTATTTCTG***TTC***ATGAT -3'	-
STAT3 to *SLCO1B3*-171	Forward:5'-ACATAATGTGTACATTCTGAGA-3'	184
	Reverse: 5'-ACTTTAAATGGTTAGTTGGCTT-3'	
STAT3 to *SLCO1B3*-215	Forward:5'-TGCTAATGTAACATGTAGGGAC-3'	169
	Reverse: 5'-ATAAATTATTTCTGGGAATGA-3'	
STAT3 to *SLCO1B3*-1268	Forward:5'-TCCCTCCACACTCCGGTTC-3'	120
	Reverse:5'-TCGGCCTCCCAAAGTGCTA-3'	
ChIP for positive control (*GAPDH*)	Forward:5'-TACTAGCGGTTTTACGGGCG-3'	166
	Reverse: 5'-TCGAACAGGAGGAGCAGAGAGCGA-3'	

Note: The underlined bases in the primers of pGL3- *SLCO1B3* are adapters containing NheI and HindIII sequences.
Bp, Base pairs; F, forward; MUT, mutated; R, reverse.

Luciferase Reporter Assays

Human hepatoma PLC/PRF/5 cell line (ATCC) and PLC/PRF/5-*ASBT* cells were used as described previously.[23] The pcDNA3.1-*STAT3* plasmid for STAT3 overexpression (*STAT3 o/e*) was generated by Hunan Fenghui Biotechnology (Changsha, China). The pGL3-basic vectors containing human *SLCO1B3* proximal promoter (about 2.0 kb upstream sequence of the translation initiation site) or its truncated forms (−1967, −261 to +25) were generated by cloning the specific PCR products that were obtained using different primers in Table 6. The pGL3-261/+25 was used to generate pGL3-*SLCO1B3* 261MUT harboring mutations in a key motif of the potential STAT3 binding within the *SLCO1B3* promoter region (Figure 7). Individual types of plasmids were co-transfected with pcDNA3.1-*STAT3 o/e* or control vector into PLC5/PRF/5 cells. One day later, the cells were treated with phosphate buffered saline or 100 ng/mL IL-6 for 12 hours. The harvested cells were lysed using 1 × passive lysis buffer, and the luciferase activity in individual groups of cells was measured by luciferase reporter assays using the Dual Luciferase Assay kit (Cat#E1910, Promega Corp), according to the protocol reported.[23]

RNA Extraction, Reverse Transcription, and RT-qPCR

Total RNA was extracted from individual groups of cells or tissues using Trizol reagent (Invitrogen), following the manufacturer's instructions. The extracted RNAs (1 μg each type of sample) were reverse-transcribed, and the relative levels of individual targeted gene mRNA transcripts were quantified by RT-qPCR using TaqMan probes and compared with the control GAPDH (Life Technologies), SYBR mixture, and the primers in Table 7.[23,28]

Western Blot Analysis

The relative levels of protein expression and phosphorylation in liver tissue homogenates, whole cell lysates, and nuclear extracts were quantified by Western blot assays.[17,23,28] Briefly, individual samples (20 μg/lane) were resolved by SDS-PAGE and transferred onto 0.22 μm PVDF membranes, followed by incubating with primary antibodies (Table 8).

ChIP Assays

Binding of STAT3 to the *SLCO1B3* promoter was analyzed by ChIP assays using a commercial ChIP Assay Kit (Millipore), according to the manufacturer's instructions.[23] Briefly, soluble chromatins were isolated from cultured cells and human livers and reacted with antibodies against STAT3 (Table 8). The precipitated DNA was amplified by PCR using the primers, and the sizes of the amplicon are listed in Table 6.

Measurement of IL-6, IL-8, IL-1β, and TNFα

The levels of IL-6, IL-8, IL-1β, or TNFα in the serum samples from patients (n = 13 for control patients and n = 39 for patients with OC) and in the supernatant of co-cultured cells were quantified using the corresponding commercial ELISA Kit (R&D Systems), according to the manufacturer's instructions.

Statistical Analysis

All data were statistically analyzed using GraphPad Prism software, version 7.0. Data are expressed as mean ± standard deviation or standard error. Comparisons between the groups were done using the independent samples *t* test or the Mann-Whitney *U* test where applicable. Comparison among multiple groups was performed using ordinary 1-way analysis of variance or Kruskal-Wallis test. All

Table 7. The Sequences of Probes (TaqMan) and Primers (SYBR) for qPCR

Gene	Sequences (5'-3')	Species/source
GAPDH	Proprietary to ABI	Human/Hs02758991_g1
SLCO1B3/OATP1B3	Proprietary to ABI	Human/Hs00251986_m1
CCL2/MCP1	Proprietary to ABI	Human/Hs00234140_m1
CXCL2	Forward:5'-CGCATCGCCCATGGTTAAGA-3'	Human/Primers (SYBR)
	Reverse:5'- ACTTTTTAGGGGGCAGACGC-3'	NC_000004.12
Gapdh	Proprietary to ABI	Mouse/Mm99999915_g1
Ccl2/Mcp1	Proprietary to ABI	Mouse/Mm00441242_m1
Cxcl2	Forward: 5'-AGGCATCTGCTTCGGGGACTCTGGC-3'	Mouse/Primers (SYBR)
	Reverse: 5'-GCAAACTCAGCCACAGGGGCGAAGG-3'	NM_015779.2
Bsep	Proprietary to ABI	Mouse/Mm00445168_m1
Mdr1b	Proprietary to ABI	Mouse/Mm00440736_m1
Ntcp	Proprietary to ABI	Mouse/Mm00441421_m1
Oatp1a1	Proprietary to ABI	Mouse/Mm01267415_m1
Cyp7b1	Proprietary to ABI	Mouse/Mm00484157_m1
Cyp27a1	Proprietary to ABI	Mouse/Mm00470430_m1
Cyp2b10	Proprietary to ABI	Mouse/Mm01972453_s1
Cyp3a11	Proprietary to ABI	Mouse/Mm00731567_m1
Fxr	Proprietary to ABI	Mouse/Mm00436425_m1
Rxrα	Proprietary to ABI	Mouse/Mm00441185_m1
sRarα	Proprietary to ABI	Mouse/Mm01296312_m1
Tnfα	Proprietary to ABI	Mouse/Mm00443258_m1
IL1β	Proprietary to ABI	Mouse/Mm00434228_m1
IL6	Proprietary to ABI	Mouse/Mm00446190_m1
Icam1	Proprietary to ABI	Mouse/Mm00516023_m1
Mcp1	Proprietary to ABI	Mouse/Mm00441242_m1
α-Sma	Proprietary to ABI	Mouse/Mm01546133_m1
Cola1	Proprietary to ABI	Mouse/Mm00801666_g1
Cola2	Proprietary to ABI	Mouse/Mm00483888_m1
Mmp2	Proprietary to ABI	Mouse/Mm00439498_m1
Ck19	Proprietary to ABI	Mouse/Mm00492980_m1
Tgfβ1	Proprietary to ABI	Mouse/Mm01178820_m1
Tgfβ2	Proprietary to ABI	Mouse/Mm00436955_m1
Tgfβ3	Proprietary to ABI	Mouse/Mm00436960_m1

ABI, Applied Biosystems; qPCR, quantitative polymerase chain reaction.

Table 8. Antibodies for Western Blot and Chromatin Co-immunoprecipitation

Antigens	Host	Company/Catalog number	Antibody dilution
GAPDH	Rabbit	Proteintech, Chicago, IL/10494-1-AP	WB 1:5000
SLCO1B3/OATP1B3	Rabbit	Sigma, Aldrich, SAB1305233	WB 1:1000
SLC10A1/NTCP	Rabbit	BOSTER, California, BA1674	WB 1:500-1:2000
Lamin A	Rabbit	Abcam, Cambridge, MA/ab26300	WB 1:10000
Phospho-STAT3	Rabbit	Cell signaling, Beverly, MA/#9145	WB 1:2000
STAT3	Rabbit	Cell signaling, Beverly, MA/#12640	WB 1:1000
EGR1	Rabbit	AffinityBiosciences, Ohio, AF0589	WB 1:1000
STAT3	Mouse	Cell signaling, Beverly, MA/#9139S	ChIP 2μg per sample

experiments were repeated at least 3 times. A *P*-value *of* $<$ .05 was considered statistically significant.

References

1. Wagner M, Zollner G, Trauner M. New molecular insights into the mechanisms of cholestasis. J Hepatol 2009; 51:565–580.
2. Arias IM, Alter HJ, Boyer JL, et al. The liver: biology and pathobiology. In: Adaptive Regulation of Hepatocyte Transporters in Cholestasis. Fifth Edition. Wiley, 2009:681–703.
3. Klaassen CD, Aleksunes LM. Xenobiotic, bile acid, and cholesterol transporters: function and regulation. Pharmacol Rev 2010;62:1–96.
4. Jung D, Podvinec M, Meyer UA, et al. Human organic anion transporting polypeptide 8 promoter is transactivated by the farnesoid X receptor/bile acid receptor. Gastroenterology 2002;122:1954–1966.
5. Durmus S, van Hoppe S, Schinkel A. The impact of organic anion-transporting polypeptides (OATPs) on disposition and toxicity of antitumor drugs: insights from knockout and humanized mice. Drug Resist Updat 2016; 27:72–88.
6. Suga T, Yamaguchi H, Sato T, et al. Preference of conjugated bile acids over unconjugated bile acids as substrates for OATP1B1 and OATP1B3. PLoS One 2017;12: e0169719.
7. Ismair MG, Stieger B, Cattori V, et al. Hepatic uptake of cholecystokinin octapeptide by organic anion-transporting polypeptides OATP4 and OATP8 of rat and human liver. Gastroenterology 2001;121:1185–1190.
8. Briz O, Romero MR, Martinez-Becerra P, et al. OATP8/1B3-mediated cotransport of bile acids and glutathione: an export pathway for organic anions from hepatocytes? J Biol Chem 2006;281:30326–30335.
9. van de Steeg E, Stranecky V, Hartmannova H, et al. Complete OATP1B1 and OATP1B3 deficiency causes human Rotor syndrome by interrupting conjugated bilirubin reuptake into the liver. J Clin Invest 2012; 122:519–528.
10. Slijepcevic D, Kaufman C, Wichers CGK, et al. Impaired uptake of conjugated bile acids and hepatitis b virus pres1-binding in na+-taurocholate cotransporting polypeptide knockout mice. Hepatology 2015;62:207–219.
11. Vaz FM, Paulusma CC, Huidekoper H, et al. Sodium taurocholate cotransporting polypeptide (SLC10A1) deficiency: conjugated hypercholanemia without a clear clinical phenotype. Hepatology 2015;61:260–267.
12. Erlinger S. NTCP deficiency: a new inherited disease of bile acid transport. Clin Res Hepatol Gastroenterol 2015; 39:7–8.
13. Keitel V, Burdelski M, Warskulat U, et al. Expression and localization of hepatobiliary transport proteins in progressive familial intrahepatic cholestasis. Hepatology 2005;41:1160–1172.
14. Yan Z, Li E, He L, et al. Role of OATP1B3 in the transport of bile acids assessed using first-trimester trophoblasts. J Obstet Gynaecol Res 2015;41:392–401.
15. Cai SY, Ouyang X, Chen Y, et al. Bile acids initiate cholestatic liver injury by triggering a hepatocyte-specific inflammatory response. JCI Insight 2017;2:e90780.
16. Roh YS, Cho A, Cha YS, et al. Lactobacillus aggravate bile duct ligation-induced liver inflammation and fibrosis in mice. Toxicol Res 2018;34:241–247.
17. Chai J, He Y, Cai SY, et al. Elevated hepatic multidrug resistance-associated protein 3/ATP-binding cassette subfamily C 3 expression in human obstructive cholestasis is mediated through tumor necrosis factor alpha and c-Jun NH2-terminal kinase/stress-activated protein kinase-signaling pathway. Hepatology 2012; 55:1485–1494.
18. Le Vee M, Lecureur V, Stieger B, Fardel O. Regulation of drug transporter expression in human hepatocytes exposed to the proinflammatory cytokines tumor necrosis factor-alpha or interleukin-6. Drug Metab Dispos 2009;37:685–693.
19. Johnson DE, O'Keefe RA, Grandis JR. Targeting the IL-6/JAK/STAT3 signalling axis in cancer. Nat Rev Clin Oncol 2018;15:234–248.
20. Liu EH, Zheng ZN, Xiao CX, et al. IL-22 relieves sepsis-induced liver injury via activating JAK/STAT3 signaling pathway. J Biol Regul Homeost Agents 2020; 34:1719–1727.
21. Xu G, Dai M, Zheng X, Lin H, Liu A, Yang J. Cholestatic models induced by lithocholic acid and alphanaphthylisothiocyanate: different etiological mechanisms for liver injury but shared JNK/STAT3 signaling. Mol Med Rep 2020;22:1583–1593.
22. Zhang LJ, Pan Q, Zhang L, et al. Runt-related transcription factor-1 ameliorates bile acid-induced hepatic inflammation in cholestasis via JAK/STAT3 signaling. Hepatology 2023;77:1866–1881.
23. Pan Q, Zhang X, Zhang L, et al. Solute carrier organic anion transporter family member 3A1 is a bile acid efflux transporter in cholestasis. Gastroenterology 2018; 155:1578–1592.e16.
24. Kim ND, Moon JO, Slitt AL, Copple BL. Early growth response factor-1 is critical for cholestatic liver injury. Toxicol Sci 2006;90:586–595.
25. Li J, Zhu X, Zhang M, et al. Limb expression 1-like (LIX1L) protein promotes cholestatic liver injury by regulating bile acid metabolism. J Hepatol 2021;75:400–413.
26. Wang H, Zhang J, Zhang X, et al. Fluorofenidone ameliorates cholestasis and fibrosis by inhibiting hepatic Erk/-Egr-1 signaling and Tgfβ1/Smad pathway in mice. Biochim Biophys Acta Mol Basis Dis 2022:166556.
27. Liu RH, Chen CM, Xia XF, et al. Homozygous p. Ser267Phe in SLC10A1 is associated with a new type of hypercholanemia and implications for personalized medicine. Sci Rep 2017;7:9214.
28. Pan Q, Luo G, Qu J, et al. A homozygous R148W mutation in Semaphorin 7A causes progressive familial intrahepatic cholestasis. EMBO Mol Med 2021: e14563.
29. Nagy A, Gertsenstein M, Vintersten K, Behringer R. Manipulating the mouse embryo: a laboratory manual. Third Edition. Cold Spring Harbor, 2003:24.

30. Oude Elferink RP, Ottenhoff R, van Wijland M, et al. Regulation of biliary lipid secretion by mdr2 P-glycoprotein in the mouse. J Clin Invest 1995;95:31–38.
31. Ubags NDJ, Suratt BT. Isolation and characterization of mouse neutrophils. Methods Mol Biol 2018;1809:45–57.

Received October 5, 2022. Accepted April 18, 2023.

Correspondence
Address correspondence to: Jin Chai, MD, PhD, Department of Gastroenterology, Institute of Digestive Diseases of PLA, Center for Metabolic-Associated Fatty Liver Diseases and Center for Cholestatic Liver Diseases, the First Affiliated Hospital (Southwest Hospital), Third Military Medical University (Army Medical University) Chongqing, 400038, China. e-mail: jin.chai@cldcsw.org; tel: 86-23-68765331.

Acknowledgments
The authors thank our team members (Cholestatic Liver Diseases Center and Center for Metabolic-Associate Fatty Liver Disease, Southwest Hospital, Army Medical University) for their technical assistance.

CRediT Authorship Contributions
Jin Chai, MD, PhD, Prof (Conceptualization: Lead; Project administration: Equal; Writing – original draft: Lead)
Qiong Pan (Data curation: Lead; Formal analysis: Lead; Investigation: Equal; Project administration: Supporting; Writing – original draft: Supporting)
Guanyu Zhu (Data curation: Lead; Formal analysis: Supporting; Investigation: Supporting)
Ziqian Xu (Data curation: Equal; Formal analysis: Equal; Methodology: Equal)
Jinfei Zhu (Formal analysis: Equal; Investigation: Equal; Resources: Equal)
Jiafeng Ouyang (Data curation: Equal; Formal analysis: Equal; Investigation: Equal)
Yao Tong (Data curation: Equal; Formal analysis: Supporting; Investigation: Supporting)
Nan Zhao (Data curation: Supporting; Investigation: Supporting; Methodology: Supporting)
Xiaoxun Zhang (Data curation: Supporting; Methodology: Supporting)
Ying Cheng (Investigation: Supporting; Methodology: Supporting; Resources: Supporting)
Liangjun Zhang (Data curation: Supporting; Formal analysis: Supporting)
Ya Tan (Investigation: Supporting; Methodology: Supporting)
Jianwei Li (Resources: Supporting)
Chengcheng Zhang (Investigation: Supporting; Resources: Supporting)
Wensheng Chen (Conceptualization: Supporting; Supervision: Supporting)
Shi-Ying Cai (Conceptualization: Supporting; Writing – review & editing: Supporting)
James L. Boyer (Conceptualization: Supporting; Project administration: Supporting; Writing – review & editing: Supporting)

Conflicts of Interest
The authors disclose no conflicts.

Funding
This work is supported by grants from the National Natural Science Foundation of China (81922012, 32171123), the Outstanding Youth Foundation of Chongqing (cstc2021jcyj-jqX0005), the Project of Chongqing Universities Innovation/Outstanding Medical Research Group (2021cqspt01 and 414Z381/4246ZO1), and the Science Foundation of Third Military Medical University (XZ-2019-505-001), China.